Author/s:
Bagheri-Fam, S;Combes, AN;Ling, CK;Wilhelm, D

Title:
Heterozygous deletion of Sox9 in mouse mimics the gonadal sex reversal phenotype associated with campomelic dysplasia in humans

Date:
2020-12-01

Citation:
Bagheri-Fam, S., Combes, A. N., Ling, C. K. & Wilhelm, D. (2020). Heterozygous deletion of Sox9 in mouse mimics the gonadal sex reversal phenotype associated with campomelic dysplasia in humans. Human Molecular Genetics, 29 (23), pp.3781-3792. https://doi.org/10.1093/hmg/ddaa259.

Persistent Link:
https://hdl.handle.net/11343/267779

Heterozygous deletion of *Sox9* in mouse mimics the gonadal sex reversal phenotype associated with campomelic dysplasia in humans

Stefan Bagheri-Fam[1], Alexander N. Combes[1,2,3], Cheuk K Ling[1], and Dagmar Wilhelm[1,*]

1. *Department of Anatomy and Neuroscience, The University of Melbourne, Parkville, VIC 3010, Australia*
2. *Murdoch Children's Research Institute, Melbourne, VIC 3052, Australia*
3. *Current address: Department of Anatomy and Developmental Biology, Monash Biomedicine Discovery Institute, Monash University, Clayton, VIC 3800, Australia*

*Author for correspondence:

Tel: +61 3 8344 9359

Email: dagmar.wilhelm@unimelb.edu.au

Abstract

Heterozygous mutations in the human *SOX9* gene cause the skeletal malformation syndrome campomelic dysplasia which in 75% of 46,XY individuals is associated with male-to-female sex reversal. While studies in homozygous *Sox9* knockout mouse models confirmed that SOX9 is critical for testis development, mice heterozygous for the *Sox9*-null allele were reported to develop normal testes. This led to the belief that the SOX9 dosage requirement for testis differentiation is different between humans, which often require both alleles, and mice, in which one allele is sufficient. However, in prior studies, gonadal phenotypes in heterozygous *Sox9* XY mice were assessed only by either gross morphology, histological staining or analyzed on a mixed genetic background. In this study, we conditionally inactivated *Sox9* in somatic cells of developing gonads using the *Nr5a1*-Cre mouse line on a pure C57BL/6 genetic background. Section and whole-mount immunofluorescence for testicular and ovarian markers showed that XY *Sox9* heterozygous gonads developed as ovotestes. Quantitative droplet digital PCR confirmed a 50% reduction of *Sox9* mRNA as well as partial sex reversal shown by an upregulation of ovarian genes. Our data show that haploinsufficiency of *Sox9* can perturb testis development in mice, suggesting that mice may provide a more accurate model of human disorders/differences of sex development (DSD) than previously thought.

Introduction

Sex in mammals is determined chromosomally with XX individuals developing as females and XY individuals as males. The Y chromosome bears the sex determining gene *Sry* (1), which is necessary and sufficient for male development (2, 3). Expression of *Sry* in the bipotential genital ridges, the gonadal anlage, from 10.5 to 12.5 days *post coitum* (dpc) in mouse drives their differentiation into testes (4, 5). If *Sry* is not present, like in XX individuals, ovarian genes such as *Foxl2*, *Wnt4* and *Rspo1* are upregulated and ovaries will develop. Impairment of the testicular program can result in the formation of ovotestes, which in mice are characterized by testicular tissue in the center and ovarian tissue at the poles of the developing gonads (6, 7).

Sry is the founding member of the SRY-related HMG (high mobility group) box (SOX) family of transcription factors that are developmental regulators of many tissues. SRY's main function is to upregulate the related, autosomal gene *Sox9* (8, 9). Initially, *Sox9* is expressed at low levels in both XX and XY genital ridges before being up-regulated and maintained in the supporting cell lineage in the testis, the Sertoli cells (10-13). SOX9 itself functions as a strong transcriptional activator, which induces the expression of a number of downstream targets, including the genes that encode desert hedgehog (*Dhh*, (14)), prostaglandin D synthase (*Ptgds*, (15, 16)), and anti-Müllerian hormone (*Amh*, (17, 18)), all of which are important for testis development and function.

In humans, heterozygous mutations in *SOX9* cause the disorder campomelic dysplasia (CD, OMIM 114290), which is characterized by severe skeletal malformations and perinatal death (19-22). In addition to the skeletal defects, phenotypes such as absence of the olfactory bulbs as well as cardiac and renal abnormalities have been described (21), reflecting the expression of *SOX9* in numerous tissues (23, 24). Furthermore, combining the information provided by

several studies (21, 25-27), only approximately 25% of affected XY individuals have a normal male phenotype at birth, while the remaining 75% show defects in testis development or complete XY sex reversal, i.e. these patients developed as females (**Table S1**), demonstrating that SOX9 is necessary for testis and hence male development. On the other hand, duplications of the chromosomal region upstream of, or that contain, *SOX9* (17q23.1-q24.3) cause XX sex reversal (28-32), implying that SOX9 is not only necessary but also sufficient for testis development. This is phenocopied in mice with ectopic expression of a *Sox9* transgene in XX individuals resulting in testis development (33). However, in contrast to humans, heterozygous deletion of *Sox9* in mice has been believed to result in normal testis development, and instead inactivation of both *Sox9* alleles is needed to observe XY sex reversal (34-37), suggesting a difference in SOX9 dosage requirements between human and mouse. Nonetheless, these studies were limited by the use of mice on a mixed genetic background and a lack of robust molecular markers for ovarian development. We circumvented these problems by using the highly efficient *Nr5a1*-Cre mouse line to delete *Sox9* on a pure C57BL/6 genetic background, which has been shown to be more sensitive to XY sex reversal compared to mixed backgrounds (6, 38-41), as well as an antibody that avidly and specifically recognizes native mouse FOXL2 protein to mark ovarian tissue (42). We show that, in contrast to the current model, heterozygous deletion of *Sox9* in mice can disturb testis differentiation, as evidenced by the formation of ovotestes.

Results

XY Nr5a1-Cre;Sox9$^{flox/+}$ fetuses have ovotestes at 14.5 dpc

To generate mice with heterozygous and homozygous deletion of *Sox9* in somatic cells of the developing gonads on a pure C57BL/6 genetic background, we crossed the *Nr5a1*-Cre mouse line (43) with the *Sox9^{flox}* mouse line, harboring a conditional *Sox9* null allele (44). This

Nr5a1-Cre line had been generated by bacterial artificial chromosome (BAC) transgenesis (43) and had been shown to efficiently delete genes in almost all gonadal somatic cells in both XX and XY fetal gonads by 11.5 dpc (43, 45, 46). These crosses generated $Sox9^{flox/+}$ and $Sox9^{flox/flox}$ (from here on referred to as controls), $Cre/+;Sox9^{flox/+}$ (from here on referred to as *Sox9*-het), and $Cre/+;Sox9^{flox/flox}$ (from here on referred to as *Sox9*-KO). Immunofluorescence (IF) analysis on sections of 14.5 dpc fetuses using antibodies to the granulosa cell marker FOXL2 (green, granulosa cells) and to the Sertoli cell marker AMH (purple, Sertoli cells) showed, as expected, extensive AMH and no FOXL2 expression in XY controls (**Fig. 1A**). In XX controls (**Fig. 1D**) as well as XY *Sox9*-KO (**Fig. 1C**), which have been described before to show complete male-to-female sex reversal (34, 45), we detected FOXL2 but no AMH. However, surprisingly, many FOXL2-positive cells were visible in XY *Sox9*-het gonads (**Fig. 1B**). These gonads presented as typical ovotestes with testicular tissue in the center and ovarian tissue at the poles (**Fig. 1B**, arrows). In addition, we also detected many FOXL2-positive cells in the center between AMH-positive testis cords in XY *Sox9*-het gonads (**Fig. 1B**, arrowheads), but only very few in XY control gonads (**Fig. 1A**).

IF analysis of XY control, XY *Sox9*-het, XY *Sox9*-KO, and XX fetuses for the Sertoli cell marker SOX9 (**Fig. 1E-H**, green fluorescence) together with the germ cell marker DDX4 confirmed the development of ovotestes in XY *Sox9*-het gonads (**Fig. 1E-H**, purple fluorescence). XY *Sox9*-het gonads demonstrated the distribution of germ cells within cords in the testicular areas (**Fig. 1F,** arrowheads), comparable to their location in XY control gonads (**Fig. 1E)**, and scattered within ovarian areas (**Fig. 1F,** arrows), similar to germ cells in XY *Sox9*-KO (**Fig. 1G**) and XX control gonads (**Fig. 1H**). To investigate the fate of germ cells in XY control, XY *Sox9*-het and XX control gonads, we performed section IF for the meiosis marker SYCP3 (**Fig. S1A-D**, purple fluorescence) together with the Sertoli cell marker SOX9 (**Fig. S1A-D**, green fluorescence). Germ cells in an ovary enter meiosis in an

anterior-posterior wave from around 13.5 dpc, which is marked by the up-regulation of SYCP3, while germ cells in a testis will enter mitotic arrest (47-50). As expected, no SYCP3-positive cells were detected in XY control (**Fig. S1A**) in contrast to XX control gonads, in which many of the germ cells had up-regulated SYCP3, especially in the anterior half of the gonad (**Fig. S1D**). In XY *Sox9*-het gonads, a few SYCP3-positive germ cells at the anterior (**Fig. S1B**, arrowheads) or posterior (**Fig. S1C**, arrowheads) pole were detected, indicating that germ cells differentiated according to their somatic environment in *Sox9*-het ovotestes.

XY Nr5a1-Cre;Sox9$^{flox/+}$ gonads appear partially sex reversed at 11.5 dpc

Having shown that XY *Sox9*-het gonads develop as ovotestes by 14.5 dpc, we next asked at what stage ovotesticular structures are established. IF analysis of XY and XX control and XY *Sox9*-het mouse fetuses from 11.5 to 13.5 dpc for FOXL2 (green, granulosa cells) and SOX9 (purple, Sertoli cells) (**Fig. 2A-I**) showed that at 11.5 dpc SOX9 expression was detectable in both XY control and *Sox9*-het gonads (**Fig. 2A,B**). However, in *Sox9*-het gonads the number of SOX9-positive cells was reduced at the anterior pole (**Fig. 2B**). In addition, FOXL2-positive cells were detected in XX control, as well as in XY control and *Sox9*-het gonads (**Fig. 2A-C**). However, XY *Sox9*-het gonads, like XX control gonads, appeared to show a higher number of FOXL2-positive cells with stronger expression when compared to XY control gonads, especially at the anterior pole (**Fig. 2B**,**C** arrows). The lower number of SOX9-positive and higher number of FOXL2-positive cells in XY *Sox9*-het gonads suggested that they might represent ovotestes as early as 11.5dpc (**Fig. 2B)**. At 12.5 and 13.5 dpc, SOX9-positive cells have assembled into testis cords in XY control (**Fig. 2D,G**) and, to a lesser degree, in XY *Sox9*-het gonads (**Fig. 2E,H**). In contrast, while there were clear ovarian parts at the anterior and posterior pole of XY *Sox9*-het gonads, as shown by FOXL2 expression (**Fig. 2E,H**, arrows), in XY control, only a few FOXL2-positive cells were detected in between testis cords (**Fig. 2D,G**). In XX controls, FOXL2 was expressed throughout the

gonad in the medullary region (**Fig. 2F,I**), as expected. Taken together, these data showed that ovotestes in XY *Sox9*-het gonads are established very early in gonad development.

Whole mount immunofluorescence is more suitable to analyze partial sex reversal

Interestingly, the IF investigation on sagittal sections of 14.5 dpc XY *Sox9*-het gonads revealed that in some cases, depending on the position of the section analyzed, the partial sex reversal was more or less obvious (**Fig. 3A-D**). Generally, lateral sections revealed ovarian tissue at the anterior (**Fig. 3A**, arrow) and medial sections at the posterior pole (**Fig. 3C**, arrow), whereas sections through the center appeared as "normal" testes (**Fig. 3B**). Moreover, analysis of corresponding lateral or medial sections of 14.5 dpc XY *Sox9*-het gonads from six fetuses revealed variable sex reversal phenotypes, ranging from the presence of only a few FOXL2-positive cells between testis cords to obvious ovarian tissue at the poles (**Fig. 3E-G**). The latter data suggest that either sex reversal was variable, or that the gonadal areas with the highest degree of sex reversal might have been missed during sectioning.

Given that section IF did not always reveal the full extent of the sex reversal, we next performed whole mount IF to obtain a more complete picture. Whole mount IF on isolated gonads and underlying mesonephroi from XY control (n=8 fetuses; 11 gonads), XX control (n=6 fetuses; 8 gonads) and XY *Sox9*-het (n=14 fetuses; 21 gonads) mouse fetuses from 12.5 to 14.5 dpc was carried out for AMH (Sertoli cells, purple fluorescence) and FOXL2 (granulosa cells, green fluorescence) (**Fig. 4** and **movies S1-6**). Though variable, an ovotesticular phenotype with testicular tissue in the center and ovarian tissue at the gonadal poles was observed in all XY *Sox9*-het gonads investigated, whereas no ovotestes were observed in any of the 11 XY control gonads. Maximum intensity Z-projection showed at 12.5 dpc (**Fig. 4A-C**), 13.5 dpc (**Fig. 4D-F**), and 14.5 dpc (**Fig. 4G-I**) expression of AMH within testis cords in XY control (**Fig. 4A,D,G**) and in the center region of XY *Sox9*-het

ovotestes (**Fig. 4B,E,H**), but not at the poles of XY *Sox9*-het ovotestes and in XX control gonads (**Fig. 4C,F,I**). AMH expression was considerably weaker in XY *Sox9*-het ovotestes (**Fig. 4B,E**) at 12.5 dpc and 13.5 dpc when compared to XY control gonads (**Fig. 4A,D**). FOXL2 was expressed in the medullary region of XX control gonads (**Fig. 4C,F,I**), as well as at the poles of XY *Sox9*-het gonads (**Fig. 4B,E,H**). In addition, confirming our results from the section IF, FOXL2 expression was also detected in cells in between testis cords at 13.5 and 14.5 dpc in the center of not only XY *Sox9*-het (**Fig. 4E,H**, arrowheads) but also, at lower numbers, in XY control gonads (**Fig. 4D,G**, arrowheads). We quantified the sex reversal phenotype at all stages by measuring the length of the testicular area as determined by the presence of testis cord (testicular length, **Fig. 4J**) and expressing it as a percentage of total gonad length (**Fig. 4J,K**). On average, the area occupied by testis cords varied between individual samples but was significantly reduced at all stages compared to XY controls (**Fig. 4K**). In addition, we quantified the length of the ovarian tissue determined by the presence of FOXL2-positive cells relative to overall gonad length at all stages (**Fig. S2A,B**) as well as the number of FOXL2-positive cells in XY control and *Sox9*-het gonads at 14.5 dpc (**Fig. S2C**). On average, ovarian tissue was greater than a quarter of gonad length across all stages in XY *Sox9*-het gonads, and the number of FOXL2-positive cells was increased significantly by 4.5-fold in XY *Sox9*-het gonads relative to XY controls (**Fig. S2**). Taken together, these data show that all XY *Sox9*-het fetal mice developed ovotestes, however the extent of the ovarian tissue varies between individual samples. We also showed that FOXL2-positive cells were not only restricted to the poles but also present in high numbers in between testis cords. Finally, these experiments suggested that whole mount IF might be more suitable than section IF to analyze partial sex reversal.

50% of Sox9 mRNA levels are not sufficient for normal testis development

Having shown that XY *Sox9*-het gonads on a C57BL/6 background develop as ovotestes, we next aimed to determine the expression levels of marker genes for testis and ovary development in these gonads compared to XY and XX controls. Droplet digital RT-PCR (ddRT-PCR) of isolated gonads from XY control (n=5), XY *Sox9*-het (n=9), XY *Sox9*-KO (n=4) and XX control (n=3) mouse fetuses at 13.5 dpc was performed for *Sox9* (**Fig. 5A**), *Amh* (**Fig. 5B**), *Foxl2* (**Fig. 5C**) and *Wnt4* (**Fig. 5D**). This analysis demonstrated that *Sox9* mRNA expression in XY *Sox9*-het gonads was reduced to 48.6% (**Fig. 5A**) compared to XY controls, while *Amh* mRNA was reduced to 49.6% (**Fig. 5B**). This reduction is likely to be caused mainly by a reduction in expression per cell and, to a lesser extent, by the small reduction in the number of *Sox9*- and *Amh*-positive cells as shown by the quantification of the whole-mount IF data (**Fig. 4K**). In addition, the expression of the two ovarian marker genes *Foxl2* and *Wnt4* were slightly, but statistically significantly, increased in XY *Sox9*-het compared to XY control gonads (**Fig. 5C,D**).

Testes appear normal in adult XY Nr5a1-Cre;Sox9$^{flox/+}$

Next, we asked the question, what happens to ovotestes in XY *Sox9*-het mice at later stages. To this end, we first performed section (**Fig. 6A-C**) and whole mount IF analyses of XY control and *Sox9*-het (**Fig. S3A,B,D,E,G,H** and **movies S7** and **S8**) and XX control (**Fig. S2A-I**) mouse gonads at 18.5 dpc for AMH and FOXL2. As expected, AMH was expressed in Sertoli cells within testis cords in XY controls and XY *Sox9*-het gonads (**Fig. 6A,B** and **Fig. S3C,F,I**, purple fluorescence), but not in XX controls, which instead expressed FOXL2 (**Fig. 6C** and **Fig. S3G-I**, green fluorescence). Similar to earlier stages, FOXL2-positive cells were also detected in XY *Sox9*-het gonads both at the poles (arrows in **Fig. 6B** and **Fig. S3D**) and within the rete testis (RT) region (arrowheads in **Fig. 6B** and **Fig. S3E**). However, the FOXL2-positive cells at the poles no longer formed a distinct ovarian-like area; they were now intermixed with AMH-positive testis cords, which appeared disorganized (arrows in **Fig.**

6B and **Fig. S3D**). Surprisingly, even in some of the XY control gonads, we could still detect a few FOXL2-positive cells in between testis cords in the rete testis area (**Fig. 6B,** arrowhead). In addition, FOXL2 was detected in the mesenchyme surrounding the Wolffian duct (**movies S3-S8**). It should be noted that many lateral or medial sections of XY *Sox9*-het mouse gonads did not show any FOXL2-positive cells (**Fig. S3H** and **movie S8)**.

Finally, we analyzed gonads from XY control and XY *Sox9*-het mice at 3 months of age. We determined the wet weight of testes and seminal vesicles, as well as the body weight (**Fig. S3**), and calculated relative testes and seminal vesicles weight per gram body weight (**Fig. 6D,E**). There were no significant differences between XY control and XY *Sox9*-het mice in any of the measured weights (**Fig. 6D,E**; **Fig. S4**). Similarly, histological analysis using PAS staining of paraffin sections from XY control and *Sox9*-het gonads (**Fig. 6F,G**), as well as section IF for SOX9 and FOXL2 did not reveal any differences between XY control and XY *Sox9*-het gonads at 3 months of age when analyzing areas in the center of the testes (**Fig. 6H,I**). SOX9 was expressed in Sertoli cells within seminiferous tubules in gonads of both control and *Sox9*-het XY mice, without any FOXL2-positive cells detectable (**Fig. 6H,I**). In contrast, sections through the rete testes area revealed that even at 3 months of age FOXL2-positive cells were detected in one out of three XY *Sox9*-het gonads analyzed (**Fig. 6J**), but in none of the XY controls (n=3) investigated (data not shown). In summary, these results showed that the ovotesticular phenotype in XY *Sox9*-het mice is of transient nature and cannot be detected in adult gonads.

Discussion

SOX9 is a transcription factor that is important in the development of many different organs and tissues (19, 22, 34, 51-58), especially skeletal development and testis determination (34-36, 51, 59). It has been believed that humans and mice fundamentally differ in their SOX9

253 dosage requirements during testis differentiation. In humans, loss-of-function of one allele is
254 sufficient to cause partial to complete sex reversal (19, 21, 22, 60), while sex reversal in *Sox9*
255 mouse models was only observed with inactivation of both alleles (34-36). In contrast to this
256 view, we show here for the first time that heterozygous deletion of *Sox9* in fetal mouse
257 gonads can lead to partial sex reversal demonstrated by the development of ovotestes. What
258 explains the discrepancy between previously published data and the data shown here? We
259 believe that there are several possible reasons, and likely it is a combination of these, that lead
260 to these inconsistencies. These are: different combinations of Cre deleter and *Sox9*-flox mice,
261 the genetic background, and techniques available and used for the analysis, all of which are
262 elaborated in more detail below.
263
264 ***Different combinations of Cre deleter and Sox9-flox mice and the genetic background of***
265 ***mice could cause differences in testicular phenotypes***
266 Heterozygous mutations of *SOX9* in humans cause campomelic dysplasia (CMPD, OMIM
267 114290), a syndrome with severe skeletal malformations which is associated with partial to
268 complete sex reversal in about 75% of all XY patients (19, 21, 22). Analysis of a
269 corresponding mouse model with a heterozygous deletion of *Sox9* indicated that these mice
270 phenocopied the skeletal, but not the associated testicular defects of CMPD patients (35). The
271 subsequent generation and analysis of homozygous *Sox9* knockout mice turned out to be a
272 major challenge. Firstly, *Sox9* heterozygous mice die soon after birth (35). Secondly, the
273 generation of homozygous *Sox9* knockout mice using germline-specific Cre lines resulted in
274 embryonic lethality at around 11.5 dpc, just before testis differentiation (51), preventing the
275 analysis of a possible testicular phenotype *in vivo*. Eventually, the use of tissue-specific Cre
276 deleter mouse lines allowed the investigation of the role of SOX9 in testis determination and
277 differentiation, showing that its loss leads to complete XY sex reversal (34, 36), which was
278 confirmed in our study.

Over the years, several different conditional *Sox9* knockout mouse models have been generated with no reports of defects in testis development in XY *Sox9* heterozygous gonads (34, 36-38, 46). These included two different *Sox9*-floxed mouse lines and several different Cre deleter lines (details see **Table S2**). In this study, we crossed for the first time *Sox9*^{tm2Gsr} (44) with the efficient *Nr5a1:Cre* mouse line (Tg(Nr5a1-cre)2Klp, (43)). In addition, most of the previous *Sox9* constitutive or conditional mouse models were on a mixed genetic background, such as 129SvEv/C57BL/6 and 129SvEv/Swiss (35, 36, 38, 46). In contrast, our mouse model was on a pure C57BL/6 background and it is known that C57BL/6 are sensitized to XY sex reversal due to a stronger ovarian program (39). Taken together, the unique Cre/*Sox9*-flox combination on a pure C57BL/6 background is likely to be more prone to XY sex reversal than previous Cre /*Sox9*-flox combinations.

Our data show that like in humans, one copy of the *Sox9* gene is not sufficient for the normal development of fetal testes in mice on a C57BL/6 genetic background. Consistent with the deletion of one *Sox9* gene copy, *Sox9* mRNA levels in XY *Sox9*-het gonads were reduced to approximately half of that in XY control testes. However, it can be assumed that the *Sox9* expression threshold required for normal testis development in mice varies between different genetic backgrounds. For example, in a study by Gonen and colleagues (37), who analyzed mouse knockout models with variable reduced *Sox9* expression levels, this threshold was determined to be between 23% and 45%, lower than in our mouse model. Unfortunately, a direct comparison with our mouse model is not possible at this stage since no information about the genetic backgrounds of the mouse strains used was reported (37). It would be interesting to measure and compare absolute *Sox9* mRNA expression levels in both XY control and XY *Sox9*-het gonads from different laboratories to shed more light into the *Sox9*

304 expression thresholds required for mouse testis determination on different genetic
305 backgrounds.
306
307 ***A testicular phenotype might have been missed due to the availability and use of techniques***
308 In our mouse model the observed ovotestes consisted of testicular tissue in the center and
309 ovarian tissue at the poles of the gonads, which is typically found in partially sex-reversed
310 mice during early gonadal development (6). To detect the testicular and ovarian tissue we
311 used antibodies that avidly and specifically recognize native SOX9, AMH and FOXL2
312 respectively. In contrast, many of the previous *Sox9* heterozygous mouse models were
313 analyzed only by histological H&E staining and/or morphological appearance of the gonads
314 (35, 36, 38), or *Sox9*-het gonads were not examined (34, 44, 46), making it possible that an
315 ovotestes phenotype was missed in these studies. This is especially likely given that the extent
316 of the sex reversal was variable in our model, and that even when using robust molecular
317 markers, the degree of sex reversal observed depended on the plane of the section investigated
318 (**Fig. 3**). One possibility to obtain a more complete picture of the sex reversal phenotype in
319 *Sox9*-het gonads is to perform whole-mount instead of section IF, as demonstrated here.
320
321 ***Is our mouse model comparable to the testicular phenotype of human CMPD patients?***
322 CMPD (OMIM 114290) in humans is caused by heterozygous mutations of *SOX9*.
323 Combining the data from several studies (21, 25-27), approximately 64% of XY CMPD
324 patients show complete XY sex reversal (**Table S1**), a severe phenotype which was not
325 observed in our *Sox9*-het mice. Given that the genetic background plays a role in the
326 sensitivity to sex reversal in mice, it is reasonable to assume that genetic diversity in humans
327 might play a similar role. To assess this, information about possible modifier genes would be
328 needed. Modifier genes and non-coding regions on autosomes and the X chromosome that can
329 sensitize or protect individuals from sex reversal have been described in mice (61-64),

however no information is available for humans. One good candidate modifier gene in humans is *SOX8*, which, like *SOX9*, encodes a protein of the SOXE group of transcription factors (65, 66). In mice, *Sox9* and *Sox8* cooperate during testis differentiation (36). Recently, three patients with 46,XY gonadal dysgenesis have been identified, two with chromosomal rearrangements around the *SOX8* locus and one harboring a deleterious missense mutation with *SOX8* (67), suggesting that *SOX8* might also be involved in human sex determination.

Another variable that differs between human and mouse is the timescale in which the gonads develop. In mice, the genital ridges are first visible at around 10.5 dpc, *Sry* is expressed from 10.5 to 12.5 dpc (4, 13, 68) and testis cord are formed over a 24-hour period from 11.5 to 12.5 dpc (69-71), hence the main steps of testis determination happen within 48 hours. In contrast, human genital ridges develop during the 4th week of gestation (72, 73), SRY is expressed from around the 6th week (74), and testis cords form in weeks 7 to 8 (74, 75), altogether spanning four weeks in contrast to two days in mice. In mouse, it is known that SRY has to function within a tight time window to up-regulate *Sox9* expression and ensure testis differentiation (76). A similar time window might exist for SOX9 in humans. It is possible that the extended timing of gonadal development in humans may worsen defects caused by sub-optimal expression of SOX9, a hypothesis that is difficult to test at present. Stem cell models have enabled the study of differences in the timing of motor neuron differentiation in human and mouse (77). In contrast, stem cell models of gonadal development are in their infancy (78), but may ultimately provide a platform to investigate the relationship between developmental timing and gene dosage in sex determination.

Given the genetic diversity, it is not surprising that complete XY sex reversal associated with *SOX9* haploinsufficiency is not fully penetrant in humans. About 25% of XY CMPD patients present with a normal male phenotype, leaving approximately 75% of XY patients with

partial or complete sex reversal (**Table S1**) (21, 25-27). Our novel mouse model shows that XY *Sox9*-het mice on a C57BL/6 background develop ovotestes, suggesting that humans and mice might be more similar with respect to their SOX9 dosage requirements during testis determination than initially thought. The *Sox9*-heterozygous mice on a C57BL/6 background could thus be regarded as a model for the testicular defects in CMPD patients. In XY *Sox9*-het mice, fetal gonads initially develop as partially sex reversed ovotestes, with ovarian tissue adjacent to testicular tissue. Histological analyses of fetal gonads from 46,XY CMPD patients with ambiguous or female genitalia have been rarely performed, but the few studies which described these showed that these gonads were also sex reversed and presented as normal ovaries (**Table S3**) (19, 60, 79). Thus, apart from the milder sex reversal phenotype in *Sox9*-het mice, when compared to this specific group of CMPD patients, the gonadal phenotypes appear to be similar in humans and mice during fetal life.

Gonads from 46,XY CMPD patients with ambiguous or female genitalia that have been investigated after birth typically presented as dysgenic ovaries with very few primordial follicles or as streak gonads (**Table S3**) (19, 25, 27, 60, 80-82). In our mouse model, ovotestes in XY *Sox9*-het mice persisted until shortly before birth, but the ovarian regions were intermixed with AMH-positive testis cords. By three months of age, XY *Sox9*-het ovotestes had almost completely resolved and were indistinguishable from control testes. It is possible that this mimics the situation in 46,XY CMPD male patients with normally descended testes. The underlying mechanism of this is unclear but could be due to elimination of the ovarian parts by apoptosis as it had been described in a different mouse model (83).

In summary, we demonstrate that, like in humans, haploinsufficiency of *Sox9* in mice can result in gonadal sex reversal during fetal life. Our *Sox9*-het mice represent a valuable mouse model not only for 46,XY CMPD patients with normal male, ambiguous or female external

genitalia, but also for human sex reversal in general and gene dosage effects during gonadal sex determination.

Materials and Methods

Mouse strains

Sox9$^{flox/flox}$ mice (Sox9^{tm2Gsr}, (44)) on a C57BL/6 background (> 10 backcrosses) were crossed with the *Nr5a1*-Cre (Tg(Nr5a1-cre)2Klp) mouse line (43)) to obtain *Cre/+;Sox9*$^{flox/+}$ mice for analysis. To confirm complete XY sex reversal in *Sox9*-null mice, *Cre/+;Sox9*$^{flox/+}$ were backcrossed to *Sox9*$^{flox/flox}$ mice to obtain *Cre/+;Sox9*$^{flox/flox}$ mice. Fetuses were collected from timed matings with noon of the day on which the mating plug was observed designated as 0.5 days *post coitum* (dpc). For more accurate staging at 11.5 dpc and 12.5 dpc, the tail somite (ts) stage of the fetus was determined by counting the number of somites posterior to the hind limb (68) with 11.5 dpc corresponding to approximately 18 ts and 12.5 dpc to 30 ts. Genotyping analysis for *Cre* (84), the *Sox9* locus (44) and the genetic sex (85) was performed using genomic DNA isolated from tail tissue.

Protocols and use of animals were approved by the Anatomy & Neuroscience Animal Ethics Committee of the University of Melbourne (approval #1614080). All experiments were performed in accordance with relevant guidelines and regulations.

Section immunofluorescence

Mouse fetuses between 11.5 dpc and 14.5dpc or whole testes from 18.5 dpc and 3-month-old mice were fixed in 4% PFA in PBS at 4°C overnight, embedded in paraffin, sectioned at 5µm, and immunofluorescence performed as described previously (13). Primary antibodies used for this study were anti-SOX9 sheep polyclonal (1:100; (7)), anti-SOX9 rabbit polyclonal

(1:300, (13)), anti-DDX4 goat polyclonal (1:200; AF2030, R&D systems), anti-AMH goat polyclonal (1:200; sc6886, Santa Cruz), anti-AMH mouse monoclonal (1:50; MCA2246, BIO-RAD), anti-SYCP3 mouse monoclonal (1:100; ab97672, Abcam), and anti-FOXL2 rabbit polyclonal (1:300; (42)). Secondary antibodies used were donkey anti-rabbit Alexa 488, donkey anti-rabbit Alexa 568, donkey anti-goat Alexa 488, donkey anti-goat Alexa 546, donkey anti-mouse Alexa 488, and donkey anti-sheep Alexa 647 obtained from Invitrogen and used at 1:300. Images were taken with a Zeiss LSM800 confocal microscope at the Biological Optical Microscopy Platform (BOMP) at the Department of Anatomy and Neuroscience, The University of Melbourne. For section immunofluorescence, 2-4 XY control, 4-6 XY *Sox9*-het, 3 XY *Sox9* KO, and 2-3 XX control fetuses were used.

Whole-mount immunofluorescence

Whole testes between 12.5 dpc and 18.5 dpc were fixed in 4% PFA for 15 min before blocking for 2 h (for 18.5 dpc 5 h) in PBS with 0.1% Triton x-100 (PBTX) and 10% heat inactivated horse serum (Invitrogen). Samples were incubated with dilutions of the primary antibodies anti-AMH goat polyclonal (1:200; sc6886, Santa Cruz) and anti-FOXL2 rabbit polyclonal (1:300; (42)) at 4°C for two days before washing three times overnight (for 18.5 dpc 2 days) in PBTX. Samples were then incubated with the secondary antibodies donkey anti-rabbit Alexa 488 and donkey anti-goat Alexa 546 obtained from Invitrogen at 1:300 dilution for two days at 4°C before a minimum of three washes in PBTX over night (for 18.5 dpc 2 days). Samples were dehydrated in a methanol series (25%, 50%, 75%, 100%, 100%, for 15 min each) and then cleared in a 2:1 solution of Benzyl benzoate: Benzyl alcohol (Sigma). Samples were mounted in 3.5 cm glass bottom culture dishes (Mattek). All samples were imaged on a Zeiss LSM 510 META inverted confocal microscope, and optical sections were collected in 3μm steps.

The Zeiss CZI image files were viewed and analysed using Fiji, an open source image processing package based on ImageJ (86). 3D reconstructions of the gonads were created using the function *'3D projection*' with projection method 'brightest point'. Standard settings were used, but with rotation angle increment '1' instead of '10' and with the option '*Interpolate*'. The 3D projections are provided as movies with 24 frames per second (fps). Z-stack images were created using the function '*Z projection*' with projection type 'Max intensity'. Z-series of confocal images are displayed at 4 fps (12.5dpc, 13.5dpc), 6 fps (18.5 dpc), and 8 fps (14.5 dpc).

Quantification of gonad length, testicular and ovarian area lengths was performed in image analysis software Imaris (BitPlane). The 'Measurement Points' function was used to guide placement of marker points, ensuring that these markers intersect with fluorescent signal within the dataset and provide accurate point-to-point measurements within the three dimensional datasets. Markers were placed at both ends of the gonad, and at either end of the region occupied by testis cords, or FOXL2-positive cells at the gonad poles to measure gonad length, testicular and ovarian tissue length respectively. Testicular and ovarian tissue length measurements were expressed as a percent of total length for each gonad and compared between genotypes. Quantification of FOXL2-positive cells was also performed in Imaris using a trimmed 'Surface' render of the 488 channel to mask and isolate FOXL2 signal within the gonad (but not mesonephros) into a new channel. The masked FOXL2 channel was subject to background subtraction (threshold 20) and median filtering (3x3x1). A spot detection algorithm ('Spots') was then run to quantify discrete points of FOXL2+ signal. Spot results were compared to the masked and original FOXL2 channel to ensure that this measure did not grossly over or under-represent the number of FOXL2-positive cells visible in each 3D dataset. The resulting data was analysed for statistically significant differences between

459 XY control and XY *Sox9*-het groups using a two-tailed, unpaired t-test with confidence
460 intervals set at 95%.
461
462 ***Periodic acid-Schiff (PAS) staining***
463 Paraffin sections (5µm) were dewaxed in xylene and re-hydrated to water. Sections were
464 oxidized with 1% periodic acid for 5 minutes and washed with distilled water for 1 min.
465 Slides were then placed in Schiff's reagent at room temperature for 10 min and washed
466 thoroughly in running tap water for 10 min. Sections were counterstained in hematoxylin for
467 30 seconds before being washed in running water for 30 sec and dipped in Scott's tap water
468 for 30 sec. After washing in running tap water, sections were dehydrated, cleared in two
469 changes of xylene for 5 minutes each, and mounted with *DPX Mounting* Media. Images were
470 taken with the light microscope Axioskop 2 (Zeiss).
471
472 ***Quantitative droplet digital RT-PCR (ddRT-PCR)***
473 ddRT-PCR was performed as described previously (87). Gonad-only samples (mesonephroi
474 removed) at 13.5 dpc were used, which were snap-frozen in liquid nitrogen immediately after
475 dissection. RNA was isolated using the RNeasy Micro Kit (QIAGEN). 200 ng of input RNA
476 was subjected to cDNA synthesis with SuperScript III First-Strand Synthesis System for RT-
477 PCR (Invitrogen) as per manufacturer's instructions. cDNA samples were diluted with
478 RNAse-free water 1:10 to 1:1000 for expression analysis. ddPCR was performed using a
479 BioRad QX100 system. Analysis of the ddPCR data was performed with QuantaSoft analysis
480 software (BioRad). ddRT-PCR data were normalized to the expression levels of *Tbp* (88).
481
482 RT-ddPCR analyses were performed on XY control (n=5 fetuses), XY *Sox9*-het (n=9 fetuses),
483 XY *Sox9* KO (n=4 fetuses), and XX control (n=3 fetuses) gonads. For each gene, data sets
484 were analyzed for statistically significant differences between XY control and XY *Sox9*-het

485 expression levels using a two-tailed, unpaired t-test with confidence intervals set at 95%.
486 Predesigned qPCR assays were used (Integrated DNA technologies (IDT)).
487
488 **Funding**
489 This work was supported by research grants from the Australian Research Council
490 [DP150101448, DP170100045 to D.W.; DE150100652 to A.N.C.] and National Health and
491 Medical Research Council of Australia [APP1156567 to A.N.C.].
492
493 **Acknowledgements**
494 Processing and sectioning were performed at the Melbourne Histology Platform, University
495 of Melbourne, and confocal microscopy was performed at the Biological Optical Microscopy
496 Platform at the Department of Anatomy and Neuroscience, University of Melbourne and at
497 the Murdoch Children's Research Institute.
498
499 **Conflict of Interest Statement**
500 The authors declare that they have no competing interests.
501
502

503 **References**

504 1 Gubbay, J., Collignon, J., Koopman, P., Capel, B., Economou, A., Münsterberg, A.,
505 Vivian, N., Goodfellow, P. and Lovell-Badge, R. (1990) A gene mapping to the sex-
506 determining region of the mouse Y chromosome is a member of a novel family of
507 embryonically expressed genes. *Nature*, **346**, 245-250.
508 2 Kato, T., Miyata, K., Sonobe, M., Yamashita, S., Tamano, M., Miura, K., Kanai, Y.,
509 Miyamoto, S., Sakuma, T., Yamamoto, T. *et al.* (2013) Production of Sry knockout mouse
510 using TALEN via oocyte injection. *Sci Rep*, **3**, 3136.
511 3 Koopman, P., Gubbay, J., Vivian, N., Goodfellow, P. and Lovell-Badge, R. (1991)
512 Male development of chromosomally female mice transgenic for Sry. *Nature*, **351**, 117-121.
513 4 Bullejos, M. and Koopman, P. (2001) Spatially dynamic expression of Sry in mouse
514 genital ridges. *Dev Dyn*, **221**, 201-205.
515 5 Koopman, P., Munsterberg, A., Capel, B., Vivian, N. and Lovell-Badge, R. (1990)
516 Expression of a candidate sex-determining gene during mouse testis differentiation. *Nature*,
517 **348**, 450-452.
518 6 Eicher, E.M., Washburn, L.L., Whitney, J.B., 3rd and Morrow, K.E. (1982) Mus
519 poschiavinus Y chromosome in the C57BL/6J murine genome causes sex reversal. *Science*
520 *(New York, N.Y*, **217**, 535-537.
521 7 Wilhelm, D., Washburn, L.L., Truong, V., Fellous, M., Eicher, E.M. and Koopman, P.
522 (2009) Antagonism of the testis- and ovary-determining pathways during ovotestis
523 development in mice. *Mech Dev*, **126**, 324-336.
524 8 Gonen, N., Futtner, C.R., Wood, S., Garcia-Moreno, S.A., Salamone, I.M., Samson,
525 S.C., Sekido, R., Poulat, F., Maatouk, D.M. and Lovell-Badge, R. (2018) Sex reversal
526 following deletion of a single distal enhancer of Sox9. *Science (New York, N.Y*, **360**, 1469-
527 1473.
528 9 Sekido, R. and Lovell-Badge, R. (2008) Sex determination involves synergistic action
529 of SRY and SF1 on a specific Sox9 enhancer. *Nature*, **453**, 930-934.
530 10 Kent, J., Wheatley, S.C., Andrews, J.E., Sinclair, A.H. and Koopman, P. (1996) A
531 male-specific role for SOX9 in vertebrate sex determination. *Development*, **122**, 2813-2822.
532 11 Morais da Silva, S., Hacker, A., Harley, V., Goodfellow, P., Swain, A. and Lovell-
533 Badge, R. (1996) *Sox9* expression during gonadal development implies a conserved role for
534 the gene in testis differentiation in mammals and birds. *Nature Genetics*, **14**, 62-68.
535 12 Sekido, R., Bar, I., Narvaez, V., Penny, G. and Lovell-Badge, R. (2004) SOX9 is up-
536 regulated by the transient expression of SRY specifically in Sertoli cell precursors. *Dev Biol*,
537 **274**, 271-279.
538 13 Wilhelm, D., Martinson, F., Bradford, S., Wilson, M.J., Combes, A.N., Beverdam, A.,
539 Bowles, J., Mizusaki, H. and Koopman, P. (2005) Sertoli cell differentiation is induced both
540 cell-autonomously and through prostaglandin signaling during mammalian sex determination.
541 *Dev Biol*, **287**, 111-124.
542 14 Li, Y., Zheng, M. and Lau, Y.F. (2014) The sex-determining factors SRY and SOX9
543 regulate similar target genes and promote testis cord formation during testicular
544 differentiation. *Cell Rep*, **8**, 723-733.
545 15 Moniot, B., Declosmenil, F., Barrionuevo, F., Scherer, G., Aritake, K., Malki, S.,
546 Marzi, L., Cohen-Solal, A., Georg, I., Klattig, J. *et al.* (2009) The PGD2 pathway,
547 independently of FGF9, amplifies SOX9 activity in Sertoli cells during male sexual
548 differentiation. *Development*, **136**, 1813-1821.
549 16 Wilhelm, D., Hiramatsu, R., Mizusaki, H., Widjaja, L., Combes, A.N., Kanai, Y. and
550 Koopman, P. (2007) SOX9 regulates prostaglandin D synthase gene transcription in vivo to
551 ensure testis development. *The Journal of biological chemistry*, **282**, 10553-10560.

552 17 Arango, N., Lovell-Badge, R. and Behringer, R. (1999) Targeted mutagenesis of the
553 endogenous mouse *Mis* gene promoter: In vivo definition of genetic pathways of vertebrate
554 sexual development. *Cell*, **99**, 409-419.
555 18 de Santa Barbara, P., Bonneaud, N., Boizet, B., Desclozeaux, M., Moniot, B.,
556 Südbeck, P., Scherer, G., Poulat, F. and Berta, P. (1998) Direct interaction of SRY-related
557 protein SOX9 and steroidogenic factor 1 regulates transcription of the human anti-Müllerian
558 hormone gene. *Molecular and Cellular Biology*, **18**, 6653-6665.
559 19 Foster, J.W., Dominguez-Steglich, M.A., Guioli, S., Kwok, C., Weller, P.A.,
560 Stevanovic, M., Weissenbach, J., Mansour, S., Young, I.D., Goodfellow, P.N. *et al.* (1994)
561 Campomelic dysplasia and autosomal sex reversal caused by mutations in an SRY-related
562 gene. *Nature*, **372**, 525-530.
563 20 Hall, B.D. and Spranger, J.W. (1980) Campomelic dysplasia. Further elucidation of a
564 distinct entity. *Am J Dis Child*, **134**, 285-289.
565 21 Mansour, S., Hall, C.M., Pembrey, M.E. and Young, I.D. (1995) A clinical and
566 genetic study of campomelic dysplasia. *J Med Genet*, **32**, 415-420.
567 22 Wagner, T., Wirth, J., Meyer, J., Zabel, B., Held, M., Zimmer, J., Pasantes, J.,
568 Bricarelli, F.D., Keutel, J., Hustert, E. *et al.* (1994) Autosomal sex reversal and campomelic
569 dysplasia are caused by mutations in and around the *SRY*-related gene *SOX9*. *Cell*, **79**, 1111-
570 1120.
571 23 Wright, E., Hargrave, M.R., Christiansen, J., Cooper, L., Kun, J., Evans, T.,
572 Gangadharan, U., Greenfield, A. and Koopman, P. (1995) The *Sry*-related gene *Sox-9* is
573 expressed during chondrogenesis in mouse embryos. *Nature Genetics*, **9**, 15-20.
574 24 Ng, L.-J., Wheatley, S., Muscat, G.E.O., Conway-Campbell, J., Bowles, J., Wright, E.,
575 Bell, D.M., Tam, P.P.L., Cheah, K.S.E. and Koopman, P. (1997) SOX9 binds DNA, activates
576 transcription and co-expresses with type II collagen during chondrogenesis in the mouse.
577 *Developmental Biology*, **183**, 108-121.
578 25 Houston, C.S., Opitz, J.M., Spranger, J.W., Macpherson, R.I., Reed, M.H., Gilbert,
579 E.F., Herrmann, J. and Schinzel, A. (1983) The campomelic syndrome: review, report of 17
580 cases, and follow-up on the currently 17-year-old boy first reported by Maroteaux et al in
581 1971. *Am J Med Genet*, **15**, 3-28.
582 26 Kwok, C., Goodfellow, P.N. and Hawkins, J.R. (1996) Evidence to exclude SOX9 as
583 a candidate gene for XY sex reversal without skeletal malformation. *J Med Genet*, **33**, 800-
584 801.
585 27 Meyer, J., Sudbeck, P., Held, M., Wagner, T., Schmitz, M.L., Bricarelli, F.D.,
586 Eggermont, E., Friedrich, U., Haas, O.A., Kobelt, A. *et al.* (1997) Mutational analysis of the
587 SOX9 gene in campomelic dysplasia and autosomal sex reversal: lack of genotype/phenotype
588 correlations. *Hum Mol Genet*, **6**, 91-98.
589 28 Benko, S., Gordon, C.T., Mallet, D., Sreenivasan, R., Thauvin-Robinet, C.,
590 Brendehaug, A., Thomas, S., Bruland, O., David, M., Nicolino, M. *et al.* (2011) Disruption of
591 a long distance regulatory region upstream of SOX9 in isolated disorders of sex development.
592 *J Med Genet*, **48**, 825-830.
593 29 Cox, J.J., Willatt, L., Homfray, T. and Woods, C.G. (2011) A SOX9 duplication and
594 familial 46,XX developmental testicular disorder. *N Engl J Med*, **364**, 91-93.
595 30 Croft, B., Ohnesorg, T., Hewitt, J., Bowles, J., Quinn, A., Tan, J., Corbin, V., Pelosi,
596 E., van den Bergen, J., Sreenivasan, R. *et al.* (2018) Human sex reversal is caused by
597 duplication or deletion of core enhancers upstream of SOX9. *Nat Commun*, **9**, 5319.
598 31 Huang, B., Wang, S., Ning, Y., Lamb, A. and Bartley, J. (1999) Autosomal XX sex
599 reversal caused by duplication of *SOX9*. *American Journal of Medical Genetics*, **87**, 349-353.
600 32 Kim, G.J., Sock, E., Buchberger, A., Just, W., Denzer, F., Hoepffner, W., German, J.,
601 Cole, T., Mann, J., Seguin, J.H. *et al.* (2015) Copy number variation of two separate

602 regulatory regions upstream of SOX9 causes isolated 46,XY or 46,XX disorder of sex
603 development. *J Med Genet*, **52**, 240-247.
604 33 Vidal, V., Chaboissier, M., de Rooij, D. and Schedl, A. (2001) *Sox9* induces testis
605 development in XX transgenic mice. *Nature Genetics*, **28**, 216-217.
606 34 Barrionuevo, F., Bagheri-Fam, S., Klattig, J., Kist, R., Taketo, M.M., Englert, C. and
607 Scherer, G. (2006) Homozygous Inactivation of Sox9 Causes Complete XY Sex Reversal in
608 Mice. *Biol Reprod*, **74**, 195-201.
609 35 Bi, W., Huang, W., Whitworth, D.J., Deng, J.M., Zhang, Z., Behringer, R.R. and de
610 Crombrugghe, B. (2001) Haploinsufficiency of Sox9 results in defective cartilage primordia
611 and premature skeletal mineralization. *Proc Natl Acad Sci U S A*, **98**, 6698-6703.
612 36 Chaboissier, M.C., Kobayashi, A., Vidal, V.I., Lutzkendorf, S., van de Kant, H.J.,
613 Wegner, M., de Rooij, D.G., Behringer, R.R. and Schedl, A. (2004) Functional analysis of
614 Sox8 and Sox9 during sex determination in the mouse. *Development*, **131**, 1891-1901.
615 37 Gonen, N., Quinn, A., O'Neill, H.C., Koopman, P. and Lovell-Badge, R. (2017)
616 Normal Levels of Sox9 Expression in the Developing Mouse Testis Depend on the
617 TES/TESCO Enhancer, but This Does Not Act Alone. *PLoS genetics*, **13**, e1006520.
618 38 Bagheri-Fam, S., Sim, H., Bernard, P., Jayakody, I., Taketo, M.M., Scherer, G. and
619 Harley, V.R. (2008) Loss of Fgfr2 leads to partial XY sex reversal. *Dev Biol*, **314**, 71-83.
620 39 Munger, S.C., Aylor, D.L., Syed, H.A., Magwene, P.M., Threadgill, D.W. and Capel,
621 B. (2009) Elucidation of the transcription network governing mammalian sex determination
622 by exploiting strain-specific susceptibility to sex reversal. *Genes Dev*, **23**, 2521-2536.
623 40 Schmahl, J., Kim, Y., Colvin, J.S., Ornitz, D.M. and Capel, B. (2004) Fgf9 induces
624 proliferation and nuclear localization of FGFR2 in Sertoli precursors during male sex
625 determination. *Development*, **131**, 3627-3636.
626 41 Bogani, D., Siggers, P., Brixey, R., Warr, N., Beddow, S., Edwards, J., Williams, D.,
627 Wilhelm, D., Koopman, P., Flavell, R.A. *et al.* (2009) Loss of mitogen-activated protein
628 kinase kinase kinase 4 (MAP3K4) reveals a requirement for MAPK signalling in mouse sex
629 determination. *PLoS Biol*, **7**, e1000196.
630 42 Polanco, J.C., Wilhelm, D., Davidson, T.L., Knight, D. and Koopman, P. (2010)
631 Sox10 gain-of-function causes XX sex reversal in mice: implications for human 22q-linked
632 disorders of sex development. *Hum Mol Genet*, **19**, 506-516.
633 43 Bingham, N.C., Verma-Kurvari, S., Parada, L.F. and Parker, K.L. (2006)
634 Development of a steroidogenic factor 1/Cre transgenic mouse line. *Genesis*, **44**, 419-424.
635 44 Kist, R., Schrewe, H., Balling, R. and Scherer, G. (2002) Conditional inactivation of
636 Sox9: a mouse model for campomelic dysplasia. *Genesis*, **32**, 121-123.
637 45 Lavery, R., Chassot, A.A., Pauper, E., Gregoire, E.P., Klopfenstein, M., de Rooij,
638 D.G., Mark, M., Schedl, A., Ghyselinck, N.B. and Chaboissier, M.C. (2012) Testicular
639 differentiation occurs in absence of R-spondin1 and Sox9 in mouse sex reversals. *PLoS*
640 *genetics*, **8**, e1003170.
641 46 Lavery, R., Lardenois, A., Ranc-Jianmotamedi, F., Pauper, E., Gregoire, E.P., Vigier,
642 C., Moreilhon, C., Primig, M. and Chaboissier, M.C. (2011) XY Sox9 embryonic loss-of-
643 function mouse mutants show complete sex reversal and produce partially fertile XY oocytes.
644 *Dev Biol*, **354**, 111-122.
645 47 Bullejos, M. and Koopman, P. (2004) Germ cells enter meiosis in a rostro-caudal
646 wave during development of the mouse ovary. *Mol Reprod Dev*, **68**, 422-428.
647 48 McLaren, A. (1988) Somatic and germ-cell sex in mammals. *Philos Trans R Soc Lond*
648 *B Biol Sci*, **322**, 3-9.
649 49 Menke, D.B., Koubova, J. and Page, D.C. (2003) Sexual differentiation of germ cells
650 in XX mouse gonads occurs in an anterior-to-posterior wave. *Dev Biol*, **262**, 303-312.
651 50 Western, P.S., Miles, D.C., van den Bergen, J.A., Burton, M. and Sinclair, A.H.
652 (2008) Dynamic regulation of mitotic arrest in fetal male germ cells. *Stem Cells*, **26**, 339-347.

653 51 Akiyama, H., Chaboissier, M.C., Behringer, R.R., Rowitch, D.H., Schedl, A., Epstein,
654 J.A. and de Crombrugghe, B. (2004) Essential role of Sox9 in the pathway that controls
655 formation of cardiac valves and septa. *Proc Natl Acad Sci U S A*, **101**, 6502-6507.
656 52 Bastide, P., Darido, C., Pannequin, J., Kist, R., Robine, S., Marty-Double, C., Bibeau,
657 F., Scherer, G., Joubert, D., Hollande, F. *et al.* (2007) Sox9 regulates cell proliferation and is
658 required for Paneth cell differentiation in the intestinal epithelium. *J Cell Biol*, **178**, 635-648.
659 53 Cheung, M., Chaboissier, M.C., Mynett, A., Hirst, E., Schedl, A. and Briscoe, J.
660 (2005) The transcriptional control of trunk neural crest induction, survival, and delamination.
661 *Dev Cell*, **8**, 179-192.
662 54 Lincoln, J., Kist, R., Scherer, G. and Yutzey, K.E. (2007) Sox9 is required for
663 precursor cell expansion and extracellular matrix organization during mouse heart valve
664 development. *Dev Biol*, **305**, 120-132.
665 55 Mori-Akiyama, Y., van den Born, M., van Es, J.H., Hamilton, S.R., Adams, H.P.,
666 Zhang, J., Clevers, H. and de Crombrugghe, B. (2007) SOX9 is required for the
667 differentiation of paneth cells in the intestinal epithelium. *Gastroenterology*, **133**, 539-546.
668 56 Reginensi, A., Clarkson, M., Neirijnck, Y., Lu, B., Ohyama, T., Groves, A.K., Sock,
669 E., Wegner, M., Costantini, F., Chaboissier, M.C. *et al.* (2011) SOX9 controls epithelial
670 branching by activating RET effector genes during kidney development. *Hum Mol Genet*, **20**,
671 1143-1153.
672 57 Seymour, P.A., Freude, K.K., Tran, M.N., Mayes, E.E., Jensen, J., Kist, R., Scherer,
673 G. and Sander, M. (2007) SOX9 is required for maintenance of the pancreatic progenitor cell
674 pool. *Proc Natl Acad Sci U S A*, **104**, 1865-1870.
675 58 Stolt, C.C., Lommes, P., Sock, E., Chaboissier, M.C., Schedl, A. and Wegner, M.
676 (2003) The Sox9 transcription factor determines glial fate choice in the developing spinal
677 cord. *Genes Dev*, **17**, 1677-1689.
678 59 Bi, W., Deng, J.M., Zhang, Z., Behringer, R.R. and de Crombrugghe, B. (1999) Sox9
679 is required for cartilage formation. *Nat Genet*, **22**, 85-89.
680 60 Cameron, F.J., Hageman, R.M., Cooke-Yarborough, C., Kwok, C., Goodwin, L.L.,
681 Sillence, D.O. and Sinclair, A.H. (1996) A novel germ line mutation in SOX9 causes familial
682 campomelic dysplasia and sex reversal. *Hum Mol Genet*, **5**, 1625-1630.
683 61 Arboleda, V.A., Fleming, A., Barseghyan, H., Delot, E., Sinsheimer, J.S. and Vilain,
684 E. (2014) Regulation of sex determination in mice by a non-coding genomic region. *Genetics*,
685 **197**, 885-897.
686 62 Eicher, E.M. and Washburn, L.L. (2001) Does one gene determine whether a
687 C57BL/6J-Y(POS) mouse will develop as a female or as an hermaphrodite? *J Exp Zool*, **290**,
688 322-326.
689 63 Livermore, C., Simon, M., Reeves, R., Stevant, I., Nef, S., Pope, M., Mallon, A.M.,
690 Wells, S., Warr, N. and Greenfield, A. (2020) Protection Against XY Gonadal Sex Reversal
691 by a Variant Region on Mouse Chromosome 13. *Genetics*, **214**, 467-477.
692 64 Zhao, L., Quinn, A., Ng, E.T., Veyrunes, F. and Koopman, P. (2017) Reduced
693 Activity of SRY and its Target Enhancer Sox9-TESCO in a Mouse Species with X*Y Sex
694 Reversal. *Sci Rep*, **7**, 41378.
695 65 Bowles, J., Schepers, G. and Koopman, P. (2000) Phylogeny of the SOX family of
696 developmental transcription factors based on sequence and structural indicators. *Dev Biol*,
697 **227**, 239-255.
698 66 Schepers, G., Teasdale, R. and Koopman, P. (2002) Twenty pairs of *Sox*: extent,
699 homology, and nomenclature of the mouse and human *Sox* transcription factor gene families.
700 *Developmental Cell*, **3**, 1-20.
701 67 Portnoi, M.F., Dumargne, M.C., Rojo, S., Witchel, S.F., Duncan, A.J., Eozenou, C.,
702 Bignon-Topalovic, J., Yatsenko, S.A., Rajkovic, A., Reyes-Mugica, M. *et al.* (2018)

703 Mutations involving the SRY-related gene SOX8 are associated with a spectrum of human
704 reproductive anomalies. *Hum Mol Genet*, **27**, 1228-1240.
705 68 Hacker, A., Capel, B., Goodfellow, P. and Lovell-Badge, R. (1995) Expression of *Sry*,
706 the mouse sex determining gene. *Development*, **121**, 1603-1614.
707 69 Combes, A.N., Lesieur, E., Harley, V.R., Sinclair, A.H., Little, M.H., Wilhelm, D. and
708 Koopman, P. (2009) Three-dimensional visualization of testis cord morphogenesis, a novel
709 tubulogenic mechanism in development. *Dev Dyn*, **238**, 1033-1041.
710 70 Cool, J., Carmona, F.D., Szucsik, J.C. and Capel, B. (2008) Peritubular myoid cells
711 are not the migrating population required for testis cord formation in the XY gonad. *Sex Dev*,
712 **2**, 128-133.
713 71 Coveney, D., Cool, J., Oliver, T. and Capel, B. (2008) Four-dimensional analysis of
714 vascularization during primary development of an organ, the gonad. *Proc Natl Acad Sci U S*
715 *A*, **105**, 7212-7217.
716 72 Byskov, A.G. (1986) Differentiation of mammalian embryonic gonad. *Physiol Rev*,
717 **66**, 71-117.
718 73 Satoh, M. (1991) Histogenesis and organogenesis of the gonad in human embryos.
719 *Journal of anatomy*, **177**, 85-107.
720 74 Hanley, N., Hagan, D., Clement-Jones, M., Ball, S., Strachan, T., Salas-Cortés, L.,
721 McElreavey, K., Lindsay, S., Robson, S., Bullen, P. *et al.* (2000) *SRY*, *SOX9*, and *DAX1*
722 expression patterns during human sex determination and gonadal development. *Mechanisms*
723 *of Development*, **91**, 403-407.
724 75 Wartenberg, H., Kinsky, I., Viebahn, C. and Schmolke, C. (1991) Fine structural
725 characteristics of testicular cord formation in the developing rabbit gonad. *Journal of electron*
726 *microscopy technique*, **19**, 133-157.
727 76 Hiramatsu, R., Matoba, S., Kanai-Azuma, M., Tsunekawa, N., Katoh-Fukui, Y.,
728 Kurohmaru, M., Morohashi, K., Wilhelm, D., Koopman, P. and Kanai, Y. (2009) A critical
729 time window of Sry action in gonadal sex determination in mice. *Development*, **136**, 129-138.
730 77 Rayon, T., Stamataki, D., Perez-Carrasco, R., Garcia-Perez, L., Barrington, C.,
731 Melchionda, M., Exelby, K., Lazaro, J., Tybulewicz, V.L.J., Fisher, E.M.C. *et al.* (2020)
732 Species-specific pace of development is associated with differences in protein stability.
733 *Science (New York, N.Y*, **369**.
734 78 Rodriguez Gutierrez, D., Eid, W. and Biason-Lauber, A. (2018) A Human Gonadal
735 Cell Model From Induced Pluripotent Stem Cells. *Front Genet*, **9**, 498.
736 79 Bergeron, A., Belle, A., Sulahian, A., Lacroix, C., Chevret, S., Raffoux, E., Arnulf, B.,
737 Socie, G., Ribaud, P. and Tazi, A. (2010) Contribution of galactomannan antigen detection in
738 BAL to the diagnosis of invasive pulmonary aspergillosis in patients with hematologic
739 malignancies. *Chest*, **137**, 410-415.
740 80 Hoefnagel, D., Wuster-Hill, D.H., Dupree, W.B., Benirschke, K. and Fuld, G.L.
741 (1978) Camptomelic dwarfism associated with XY-gonadal dysgenesis and chromosome
742 anomalies. *Clin Genet*, **13**, 489-499.
743 81 Hovmoller, M.L., Osuna, A., Eklof, O., Fredga, K., Hjerpe, A., Linsten, J., Ritzen, M.,
744 Stanescu, V. and Svenningsen, N. (1977) Camptomelic dwarfism. A genetically determined
745 mesenchymal disorder combined with sex reversal. *Hereditas*, **86**, 51-62.
746 82 Rodriguez, J.I. (1993) Vascular anomalies in campomelic syndrome. *Am J Med Genet*,
747 **46**, 185-192.
748 83 Gregoire, E.P., Lavery, R., Chassot, A.A., Akiyama, H., Treier, M., Behringer, R.R.
749 and Chaboissier, M.C. (2011) Transient development of ovotestes in XX Sox9 transgenic
750 mice. *Dev Biol*, **349**, 65-77.
751 84 Lecureuil, C., Fontaine, I., Crepieux, P. and Guillou, F. (2002) Sertoli and granulosa
752 cell-specific Cre recombinase activity in transgenic mice. *Genesis*, **33**, 114-118.

753 85 McFarlane, L., Truong, V., Palmer, J.S. and Wilhelm, D. (2013) Novel PCR assay for
754 determining the genetic sex of mice. *Sex Dev*, **7**, 207-211.
755 86 Schindelin, J., Arganda-Carreras, I., Frise, E., Kaynig, V., Longair, M., Pietzsch, T.,
756 Preibisch, S., Rueden, C., Saalfeld, S., Schmid, B. *et al.* (2012) Fiji: an open-source platform
757 for biological-image analysis. *Nat Methods*, **9**, 676-682.
758 87 Shapouri, F., Saeidi, S., de Iongh, R.U., Casagranda, F., Western, P.S., McLaughlin,
759 E.A., Sutherland, J.M., Hime, G.R. and Familari, M. (2016) Tob1 is expressed in developing
760 and adult gonads and is associated with the P-body marker, Dcp2. *Cell Tissue Res*, **364**, 443-
761 451.
762 88 Svingen, T., Spiller, C.M., Kashimada, K., Harley, V.R. and Koopman, P. (2009)
763 Identification of suitable normalizing genes for quantitative real-time RT-PCR analysis of
764 gene expression in fetal mouse gonads. *Sex Dev*, **3**, 194-204.
765

766
767

768 **Figure legends**

769

770 **Figure 1. Markers of gonadal differentiation in control, XY *Sox9*-het and XY *Sox9* KO**
771 **gonads at 14.5 dpc.** (**A-D**) Double immunofluorescence on sagittal sections of paraffin-
772 embedded 14.5 dpc XY control, XY *Sox9*-het, XY *Sox9*-KO and XX control gonads for
773 FOXL2 (green, granulosa cells) and AMH (purple, Sertoli cells). Arrows point to FOXL2-
774 positive cells at the poles of the XY *Sox9*-het gonad. Arrowheads indicate FOXL2-positive
775 cells in the center of *Sox9*-het and XY control gonads. (**E-H**) Double immunofluorescence
776 (IF) on sagittal sections of paraffin-embedded 14.5 dpc XY control, XY *Sox9*-het, XY *Sox9*-
777 KO and XX control gonads for SOX9 (green, Sertoli cells) and DDX4 (purple, germ cells).
778 Arrows point to scattered germ cells at the poles of the XY *Sox9*-het gonad. Arrowheads
779 indicate germ cells inside testis cords in *Sox9*-het and XY control gonads. All images of fetal
780 gonad sections are oriented so that the anterior pole is at the top and the mesonephros is on
781 the left of the gonad. Scale bar, 100 μm.

782

783 **Figure 2. Expression analysis of FOXL2 and SOX9 in control and XY *Sox9*-het gonads**
784 **between 11.5 dpc and 13.5 dpc**. (**A-I**) Double immunofluorescence analysis on sagittal
785 sections from 11.5 dpc (**A-C**), 12.5 dpc (**D-F**) and 13.5 dpc (**G-I**) XY control, *Sox9*-het, and
786 XX control gonads for FOXL2 (green, granulosa cells) and SOX9 (purple, Sertoli cells). In all
787 images of fetal gonad sections the anterior pole is at the top and the mesonephros is on the left
788 of the gonad. Arrows point to FOXL2-positive cells at the poles of *Sox9*-het and XX control
789 gonad sections. Scale bar, 100 μm.

790

791 **Figure 3. Analysis of sex reversal in XY *Sox9*-het gonads by immunofluorescence on**
792 **sagittal sections at 14.5 dpc.** (**A-C**) Double immunofluorescence analysis on sagittal sections
793 from a single 14.5 dpc XY *Sox9*-het gonad (right gonad) for FOXL2 (green, granulosa cells)

794 and AMH (purple, Sertoli cells). The dotted lines in (**D)** indicate the position of the sections
795 analyzed in (**A-C**). Lateral and medial refers to the position within the fetus. Lateral section 1
796 and medial section 3 revealed sex reversal at the anterior and posterior poles, respectively,
797 while the center region 2 showed a normal testicular phenotype. (**E-G**) Double IF analysis on
798 corresponding lateral sections from three independent 14.5 dpc XY *Sox9*-het gonads (right
799 gonads) for FOXL2 and AMH showed a variable sex reversal phenotype. Scale bar, 100 μm.
800
801 **Figure 4. Analysis of sex reversal in XY *Sox9*-het gonads by whole mount**
802 **immunofluorescence between 12.5 dpc and 14.5 dpc.** (**A-I**) Double whole mount
803 immunofluorescence analysis of 12.5 dpc, 13.5 dpc and 14.5 dpc XY control, XY *Sox9*-het
804 and XX control gonads for AMH (purple, Sertoli cells) and FOXL2 (green, granulosa cells).
805 The images represent maximum intensity projection (Z-stacks) of the Z-series using Fiji.
806 Arrowheads point to FOXL2-positive cells between testis cords in XY control and XY *Sox9*-
807 het gonads. Scale bar, 100 μm. (**J**) Schematic representation of gonad and testicular area
808 length measurements. (**K**) Quantification of the percentage of testicular area length relative to
809 overall gonad length of XY control (solid bars) and *Sox9*-het (dashed bars) at 12.5, 13.5, and
810 14.5 dpc (unpaired two-tailed t-test; mean ± standard error of the mean).
811
812 **Figure 5. Expression analysis of testicular and ovarian markers in 13.5 dpc control, XY**
813 ***Sox9*-het and XY *Sox9*-KO gonads by droplet digital RT-PCR.** (**A-D**) mRNA expression
814 levels of *Sox9* (**A**), *Amh* (**B**), *Foxl2* (**C**) and *Wnt4* (**D**) in 13.5 dpc XY control (n=5 fetuses),
815 XY *Sox9*-het (n=9 fetuses), XY *Sox9* KO (n=4 fetuses), and XX control (n=3 fetuses) gonads.
816 Expression levels are shown relative to the expression levels of *Tbp.* XY samples are shown
817 in blue, XX in pink. *$P < 0.05$, ***$P < 0.0001$ (unpaired student t-test between XY control
818 and XY *Sox9*-het gonads). Mean ± standard error of the mean (SEM).
819

Figure 6. Ovotestes in XY *Sox9*-het gonads resolve into testes. (**A-C**) Double immunofluorescence analysis on sections from 18.5 dpc XY control, XY *Sox9*-het, and XX control gonads for FOXL2 (green, granulosa cells) and AMH (purple, Sertoli cells). The arrow in (**B**) points to the ovarian region populated with testis cords at the anterior pole of the XY *Sox9*-het gonad. Arrowheads in (**A**,**B**) indicate FOXL2-positive cells within the rete testis region in XY control and XY *Sox9*-het gonads. (**D,E**) Testis and seminal vesicle weight relative to body weight in 3 months old XY control (n=3) and XY *Sox9*-het (n=4) mice. (**F,G**) Histological analysis using Periodic acid Schiff staining of paraffin sections from XY control and *Sox9*-het gonads at 3 months of age. (**H-J**) Double immunofluorescence analysis on sections from 3 months old XY control (**H**) and XY *Sox9*-het (**I and J**) gonads for FOXL2 (green, granulosa cells) and SOX9 (purple, Sertoli cells). Images in (**H**) and (**I**) show areas from the center of the gonads, while the image in (**J**) shows an area around the rete testis. ns, not significant (unpaired student t-test; mean ± standard error of the mean (SEM); RT, rete testis. Scale bars, 100 μm.

Figure S1. Analysis of germ cell development in 14.5 dpc XY *Sox9*-het gonads. (**A-D**) Double immunofluorescence analysis on sagittal sections from 14.5 dpc XY control (**A**), XY *Sox9*-het (**B** and **C**), and XX control (**D**) gonads for SOX9 (green, Sertoli cells) and SYCP3 (purple, germ cell meiosis). Arrowheads in (**B**) and (**C**) point to germ cells that enter meiosis at the poles of XY *Sox9*-het gonads. Scale bar, 100 μm.

Figure S2. Quantification of ovarian tissue. (**A**) Schematic representation of gonad and ovarian tissue length measurements. (**B**) Quantification of the percentage of ovarian area length relative to overall gonad length of XY control (solid bars) and *Sox9*-het (dashed bars) at 12.5, 13.5, and 14.5 dpc (unpaired two-tailed t-test; mean ± standard error of the mean). (**C**) Quantification of FOXL2-positive cells in XY control (n=3) and *Sox9*-het (n=7) gonads at

14.5 dpc using whole-mount immunofluorescence analysis (unpaired student t-test; Mean ± standard error of the mean).

Figure S3. **Analysis of sex reversal in XY *Sox9*-het gonads by whole mount immunofluorescence at 18.5 dpc.** (**A-I**) Double whole mount immunofluorescence analysis of 18.5 dpc XY control, XY *Sox9*-het and XX control gonads for AMH (purple, Sertoli cells) and FOXL2 (green, granulosa cells). The three images per genotype represent corresponding optical sections from different regions of the gonads. The arrow in (**B**) indicates the ovarian region in the XY *Sox9*-het gonad. Arrowheads point to FOXL2-positive cells within the rete testis region of XY control (**D**) and XY *Sox9*-het **(E**) gonads. RT, rete testis. Scale bar, 100 μm.

Figure S3. Testis, seminal vesicle and body weight of 3 months old XY control and XY *Sox9*-het mice. (**A**) Testis weight, (**B**) seminal vesicle weight, (**C**) ratio of testis and seminal vesicle weight, and (**D**) body weight of 3 months old XY control (n=3) and XY *Sox9*-het (n=4) mice. ns, not significant (unpaired student t-test; Mean ± standard error of the mean (SEM)).

Movie S1. 3D projection of a 12.5 dpc XY control gonad. Double immunofluorescence for AMH (purple, Sertoli cells) and FOXL2 (green, granulosa cells).

Movie S2. 3D projection of a 12.5 dpc XY *Sox9*-het gonad. Double immunofluorescence for AMH (purple, Sertoli cells) and FOXL2 (green, granulosa cells).

Movie S3. 3D projection of a 13.5 dpc XY control gonad. Double immunofluorescence for AMH (purple, Sertoli cells) and FOXL2 (green, granulosa cells).

Movie S4. 3D projection of a 13.5 dpc XY *Sox9*-het gonad. Double immunofluorescence for AMH (purple, Sertoli cells) and FOXL2 (green, granulosa cells).

Movie S5. 3D projection of a 14.5 dpc XY control gonad. Double immunofluorescence for AMH (purple, Sertoli cells) and FOXL2 (green, granulosa cells).

Movie S6. 3D projection of a 14.5 dpc XY *Sox9*-het gonad. Double immunofluorescence for AMH (purple, Sertoli cells) and FOXL2 (green, granulosa cells).

Movie S7. 3D projection of an 18.5 dpc XY control gonad. Double immunofluorescence for AMH (purple, Sertoli cells) and FOXL2 (green, granulosa cells).

Movie S8. 3D projection of an 18.5 dpc XY *Sox9*-het gonad. Double immunofluorescence for AMH (purple, Sertoli cells) and FOXL2 (green, granulosa cells).

Abbreviations

Dpc - days *post coitum*; *Sox9*-het - *Cre/+;Sox9*$^{flox/+}$; *Sox9*-KO - *Cre/+;Sox9*$^{flox/flox}$

Figure 1

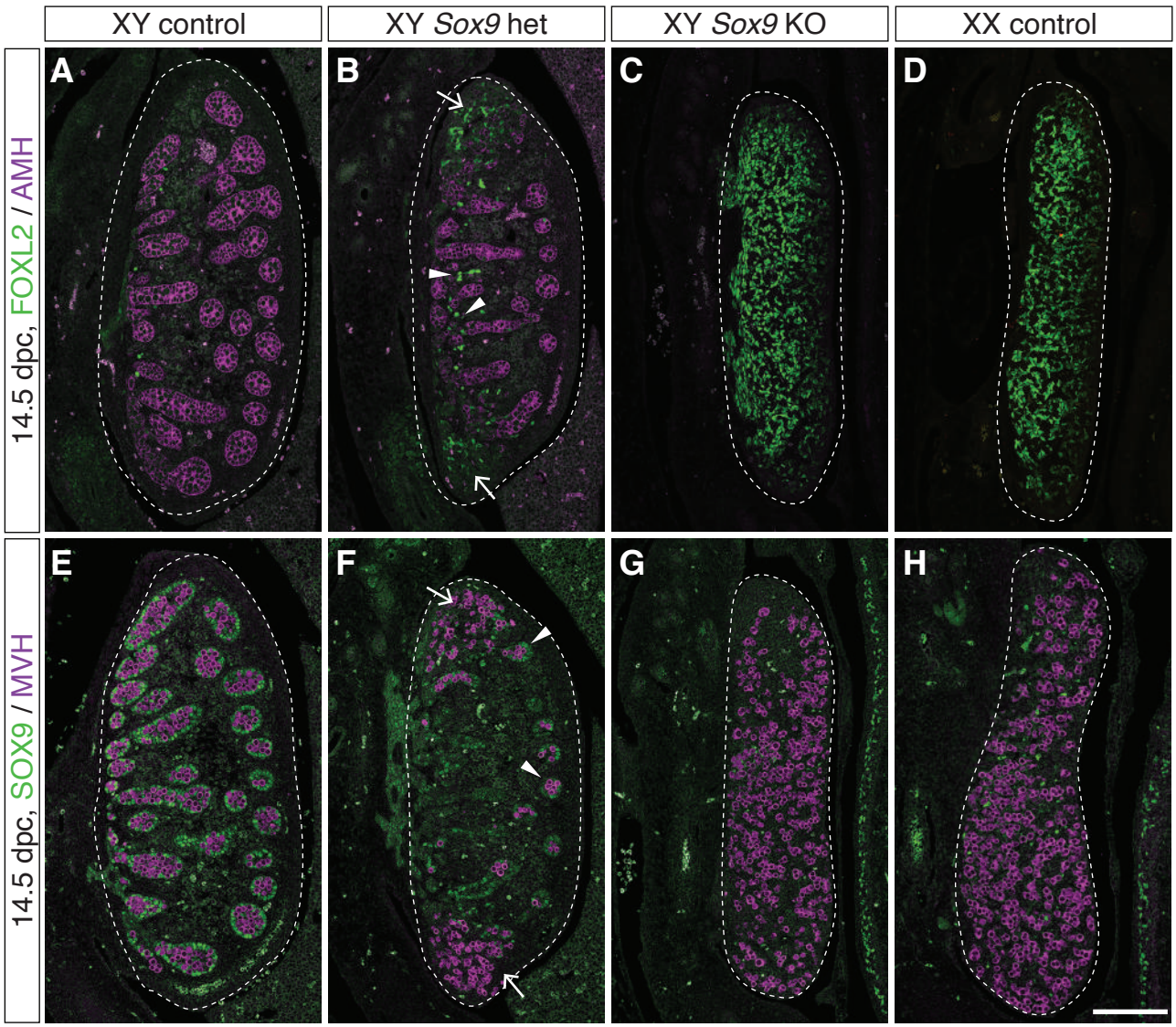
XY control
XY *Sox9* het
XY *Sox9* KO
XX control
14.5 dpc, FOXL2 / AMH
14.5 dpc, SOX9 / MVH
A
B
C
D
E
F
G
H

Figure 2

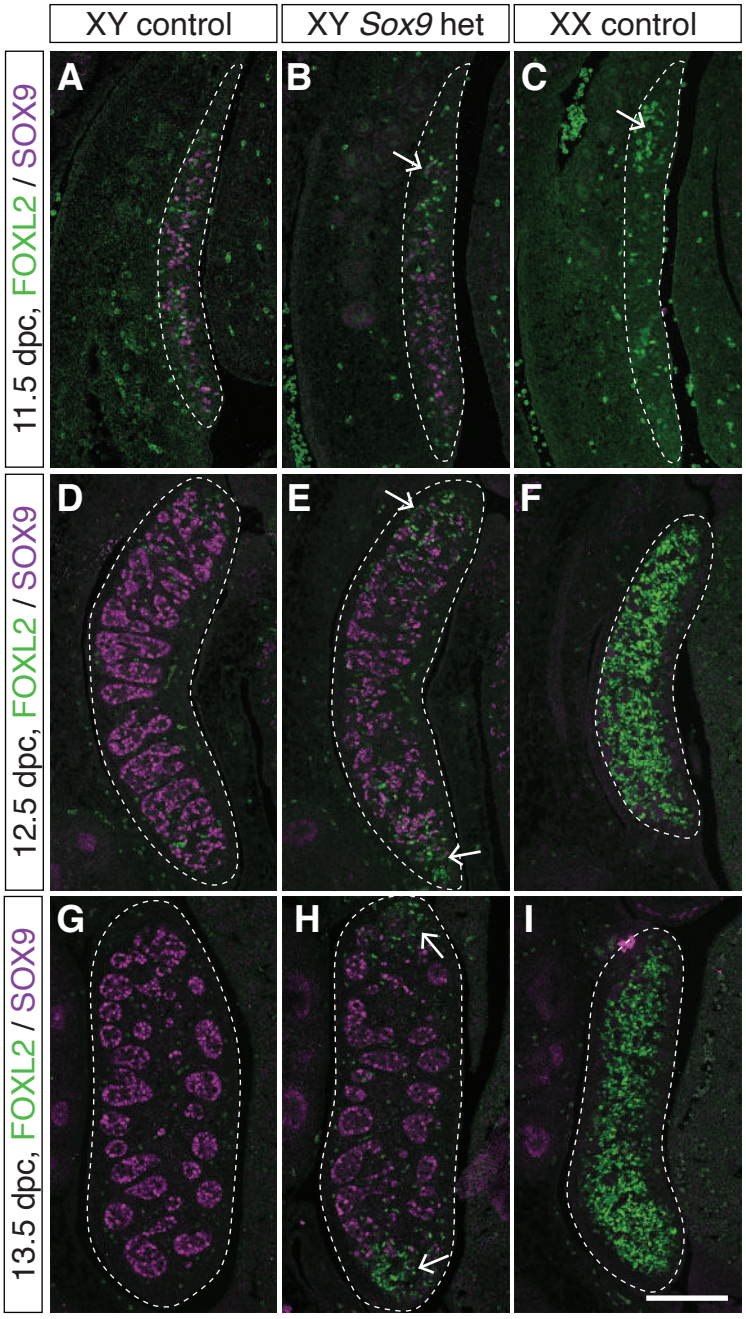
XY control
XY Sox9 het
XX control
11.5 dpc, FOXL2 / SOX9
12.5 dpc, FOXL2 / SOX9
13.5 dpc, FOXL2 / SOX9
A
B
C
D
E
F
G
H
I

Figure 3

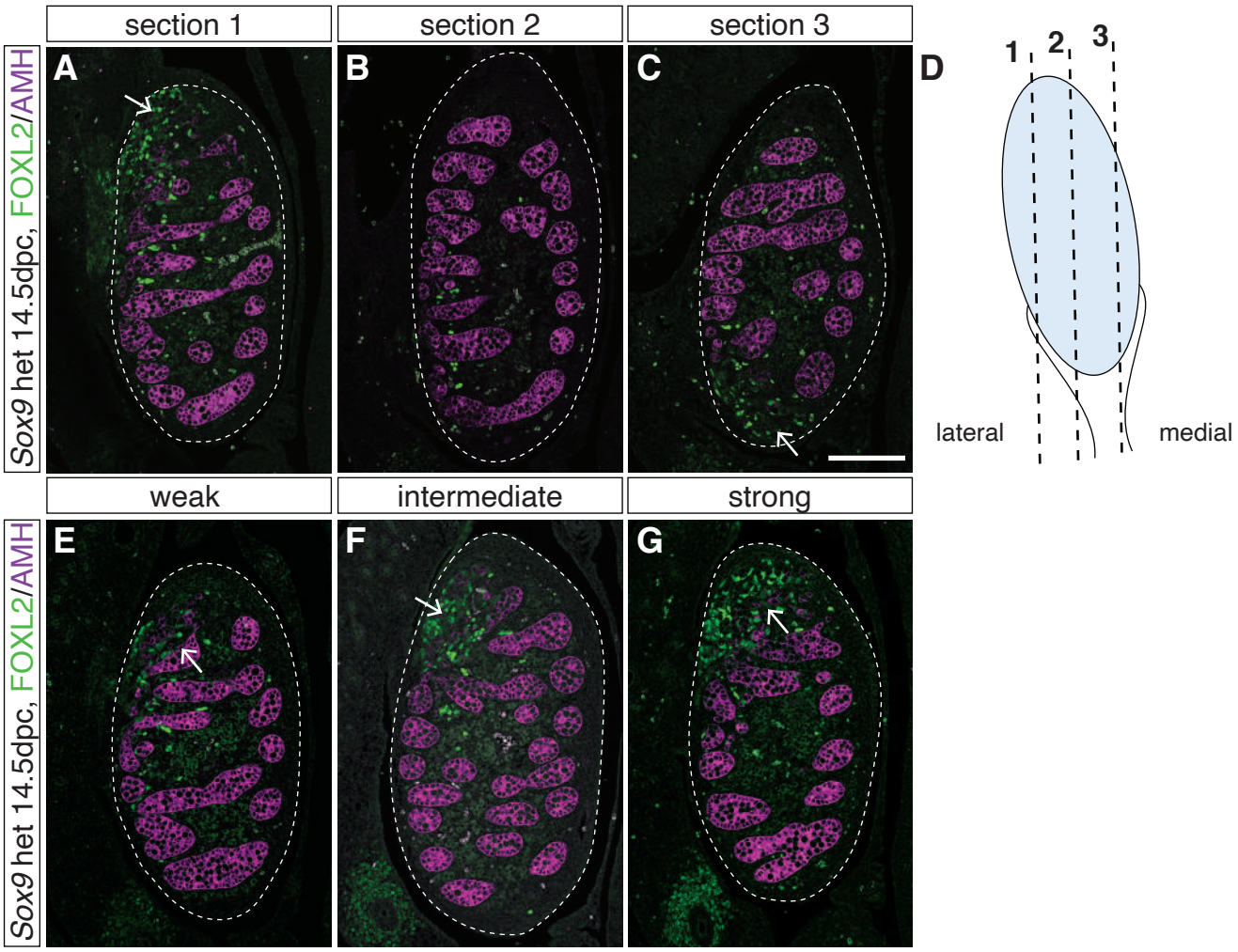
section 1
section 2
section 3
A
B
C
D
1
2
3
lateral
medial
Sox9 het 14.5dpc, FOXL2/AMH
weak
intermediate
strong
E
F
G
Sox9 het 14.5dpc, FOXL2/AMH

Figure 4

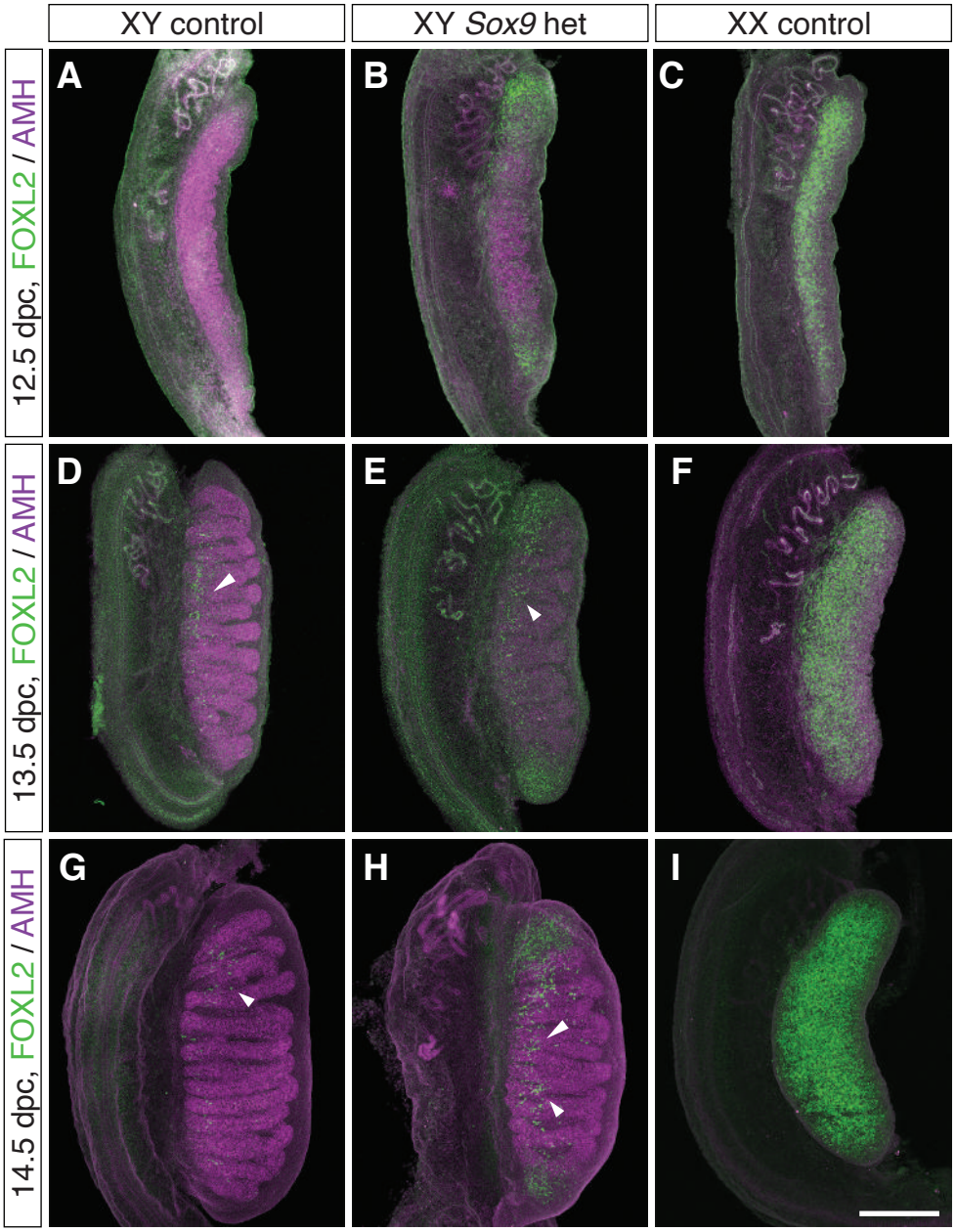
XY control
XY *Sox9* het
XX control
12.5 dpc, FOXL2 / AMH
13.5 dpc, FOXL2 / AMH
14.5 dpc, FOXL2 / AMH
A
B
C
D
E
F
G
H
I

Figure 5

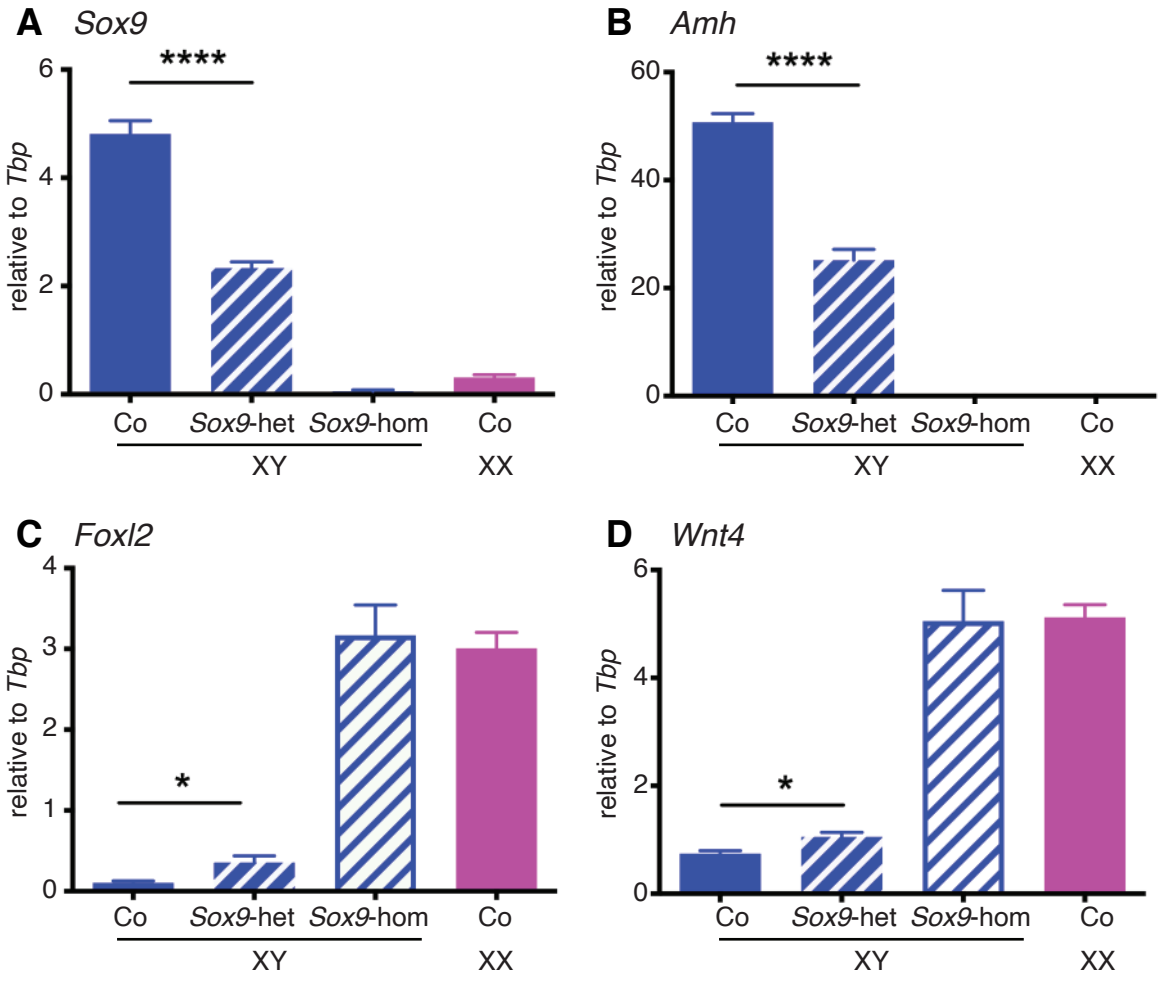
A Sox9
****
relative to Tbp
6
4
2
0
Co
Sox9-het
Sox9-hom
Co
XY
XX
B Amh
****
relative to Tbp
60
40
20
0
Co
Sox9-het
Sox9-hom
Co
XY
XX
C Foxl2
*
relative to Tbp
4
3
2
1
0
Co
Sox9-het
Sox9-hom
Co
XY
XX
D Wnt4
*
relative to Tbp
6
4
2
0
Co
Sox9-het
Sox9-hom
Co
XY
XX

Figure 6

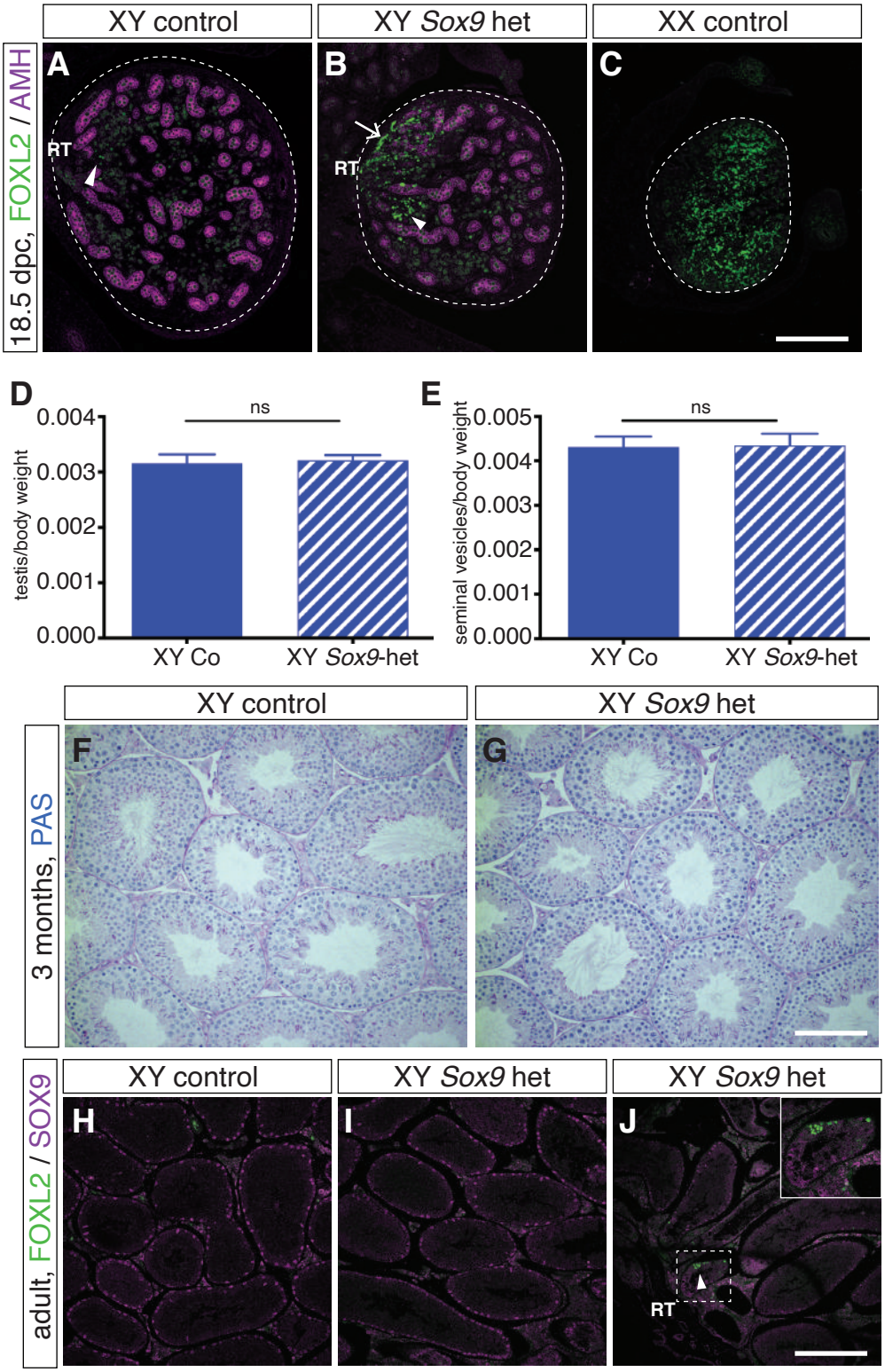
XY control
XY Sox9 het
XX control
18.5 dpc, FOXL2 / AMH
A
B
C
RT
RT
D
testis/body weight
0.004
0.003
0.002
0.001
0.000
ns
XY Co
XY Sox9-het
E
seminal vesicles/body weight
0.005
0.004
0.003
0.002
0.001
0.000
ns
XY Co
XY Sox9-het
XY control
XY Sox9 het
3 months, PAS
F
G
XY control
XY Sox9 het
XY Sox9 het
adult, FOXL2 / SOX9
H
I
J
RT

Figure S1

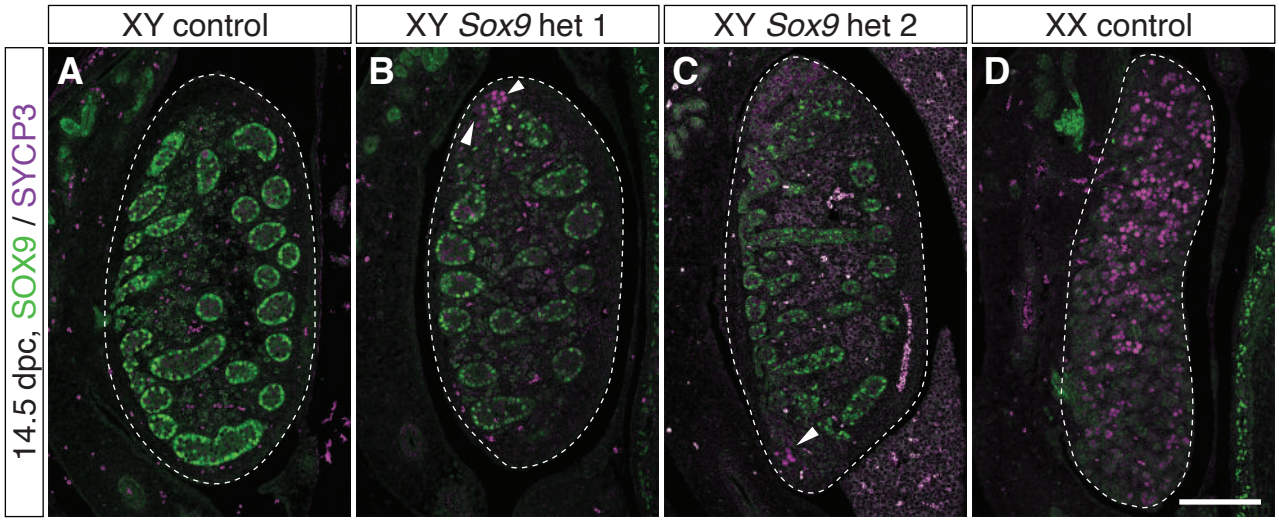
XY control
XY *Sox9* het 1
XY *Sox9* het 2
XX control
14.5 dpc, SOX9 / SYCP3
A
B
C
D

Figure 4

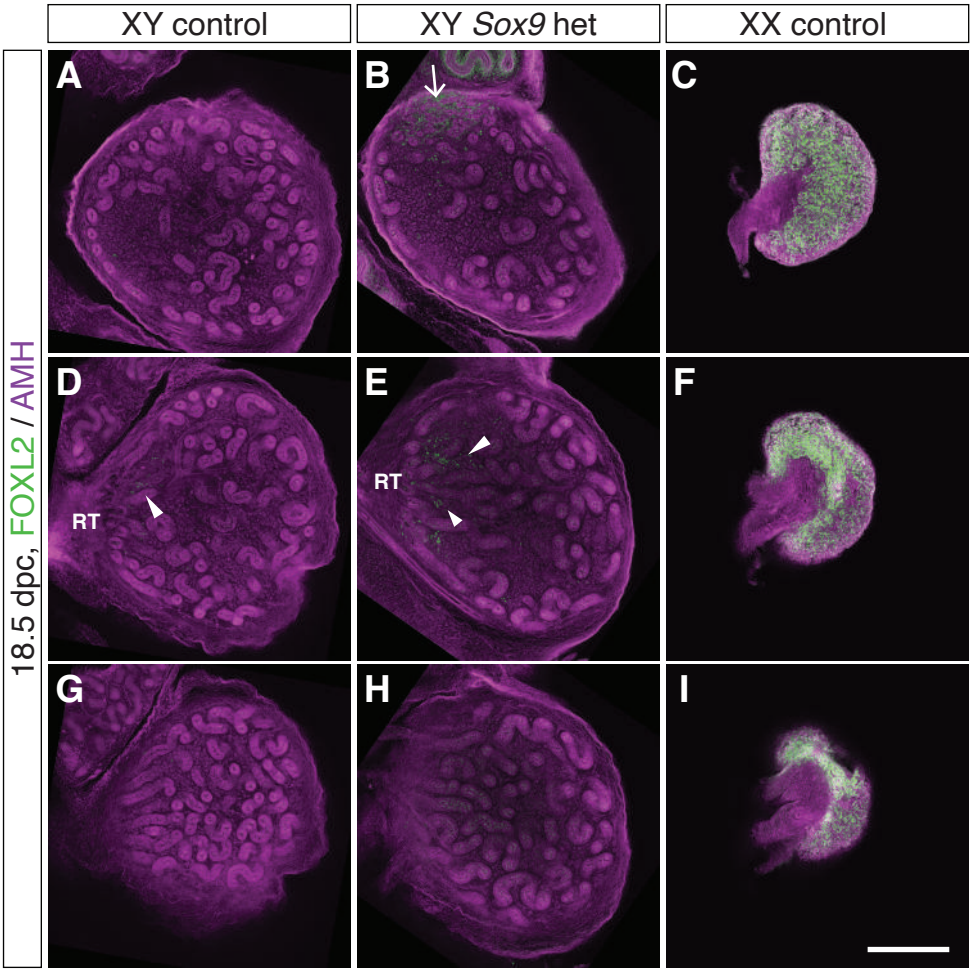
XY control
XY *Sox9* het
XX control
18.5 dpc, FOXL2 / AMH
A
B
C
D
E
F
G
H
I
RT
RT

Figure S2

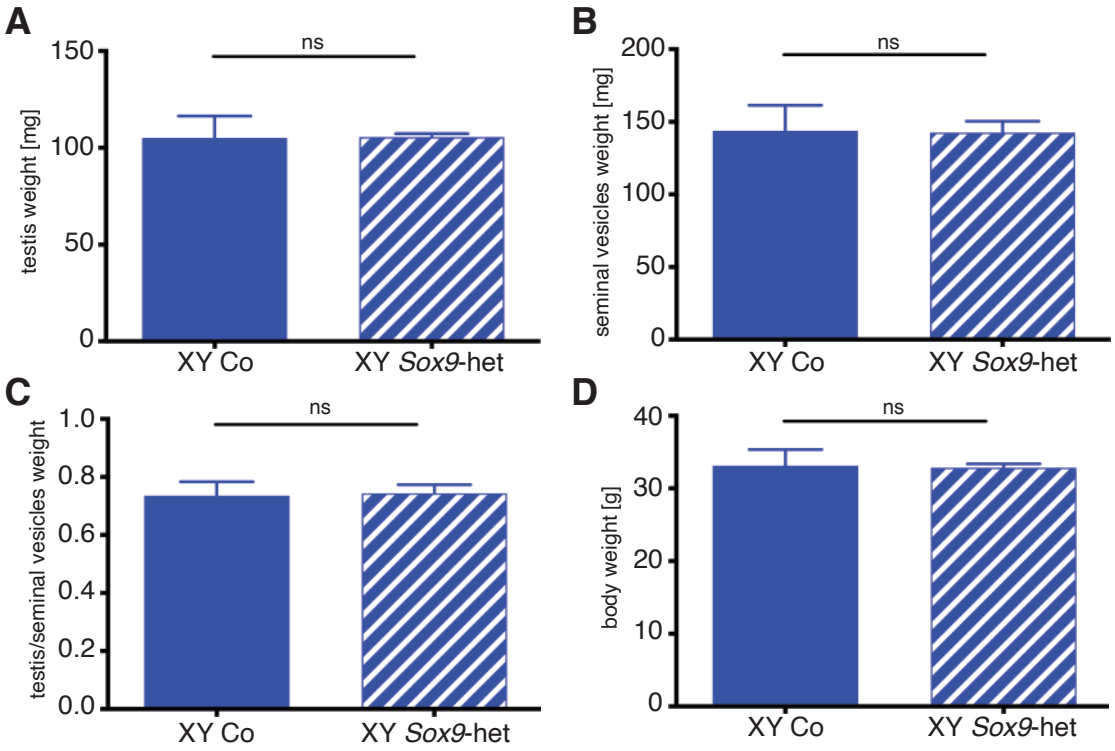
A
testis weight [mg]
150
100
50
0
ns
XY Co
XY Sox9-het
B
seminal vesicles weight [mg]
200
150
100
50
0
ns
XY Co
XY Sox9-het
C
testis/seminal vesicles weight
1.0
0.8
0.6
0.4
0.2
0.0
ns
XY Co
XY Sox9-het
D
body weight [g]
40
30
20
10
0
ns
XY Co
XY Sox9-het